

FORESIGHT

A RADIO TAGGING MISSION TO NEAR EARTH ASTEROID APOPHIS

CONCEPT SUMMARY REPORT

Submission for the Planetary Society 2007 Apophis Mission Design Competition
31 August 2007

TEAM MEMBERS

SpaceWorks Engineering, Inc. (SEI) | www.sei.aero
SpaceDev, Inc. | www.spacedev.com

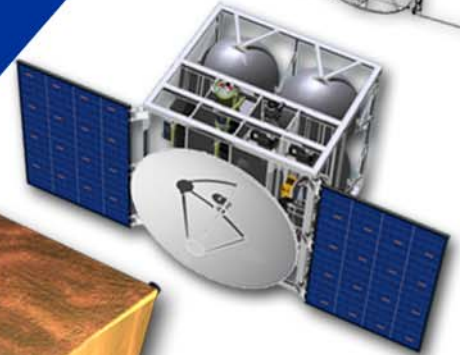
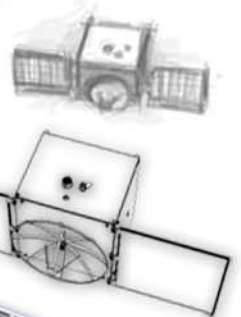


TABLE OF CONTENTS

Executive Summary	3
Nomenclature	4
I. Mission Overview	4
A. Introduction	4
B. Overall Mission Summary	6
C. Launch Opportunities	8
1. Interplanetary Trajectory Analysis	8
2. Launch Window Analysis	9
3. Delta-V Budgets	12
D. Launch Vehicle Selection	14
II. Apophis Orbit Determination and 2029 Error Ellipse Prediction	15
A. Introduction	15
B. Locating the Center of Mass of the Target Asteroid	15
C. Locating Foresight with Respect to the Earth	16
D. Approach to Error Ellipse Reduction	16
1. Orbit Propagation and Error Ellipse Estimation	16
2. Orbit Determination Method	17
3. Orbit Determination Optimizer	18
E. Measurement Frequency and Arc Length Trades	18
F. Selected Measurement Frequency and Duration	19
G. Before and After Mission Distributions on the 2029 Encounter b-plane	20
III. Spacecraft Overview	21
A. Overall Spacecraft Design	21
B. Foresight Encounter Spacecraft	22
1. Overview	22
2. Scientific Instrument Suite	27
3. Detailed Subsystem Description	28
C. Propulsive Transfer Vehicle (PTV)	32
D. Reliability Assessment	33
E. Life-Cycle Cost (LCC) Analysis	36
IV. Project Management	36
Acknowledgements	37
References	37

Foresight: A Radio Tagging Mission to Near Earth Asteroid Apophis

Mark G. Schaffer^{*}, A.C. Charania[†], John R. Olds[‡], Ben Stahl[§], Nicholas Boechler^{**}, Dominic DePasquale^{††}
SpaceWorks Engineering, Inc. (SEI), 1200 Ashwood Parkway, Suite 506, Atlanta, Georgia, 30338 USA

Jesse.Koenig^{‡‡}
SpaceDev, Inc., 13855 Stowe Drive, Poway, California 92064 USA

Executive Summary

The Foresight spacecraft is a concept design for a radio tagging mission to Near Earth Asteroid (NEO) Apophis. The spacecraft is designed to be a low-cost, low-risk, minimal science mission in order to achieve the goal of obtaining accurate tracking information for Apophis. The baseline spacecraft mission includes a launch from Wallops Island, Virginia on an Orbital Sciences Corporation Minotaur IV launch vehicle. Five launch windows have been identified spanning the years 2012 to 2014. The mission requires a chemical propulsive transfer vehicle to perform the outbound burn to Apophis (3,600 m/s) with the Foresight encounter spacecraft performing a portion of the Earth departure, and the Apophis capture burn (total less than 2,400 m/s). The mass of the Foresight spacecraft is 220 kg (propulsive transfer vehicle of 1,387 kg). The Foresight spacecraft is powered by solar arrays augmented by rechargeable batteries; the transfer vehicle is powered by onboard batteries. The Spacecraft has two main instruments, a multi-spectral imager and laser altimeter, which over a span of 300 days reduces the $\pm 3\sigma$ error ellipse of Apophis' trajectory ("keyhole" or b-place encounter) in 2029 to 6.0 kilometers by 2017. The spacecraft leverages off the shelf technologies where possible, incorporating leaner approaches to spacecraft design. The total cost for this mission is estimated to be \$137.2 M (\$94.2 M for spacecraft and instrument development and acquisition, \$21 M for operations, and \$22 M for the launch vehicle). Overall system reliability is estimated to be 90.2%. The Foresight spacecraft is a low cost asteroid spacecraft mission that can be implemented with low risk in order to obtain detailed information on the future orbital trajectory of Apophis.

* Project Engineer, mark.schaffer@sei.aero, 1+770.379.8005 [Point of Contact].

† Senior Futurist, ac@sei.aero, 1+770.379.8006.

‡ Chief Executive Officer, john.olds@sei.aero, 1+770.379.8002.

§ Graduate Intern, ben.stahl@sei.aero, 1+770.79.8000.

** Undergraduate Intern, nicholas.boechler@sei.aero, 1+770.379.8000.

†† Systems Engineer, dominic.depasquale@sei.aero, 1+770.379.8009.

‡‡ Systems Engineer, jesse.koenig@SpaceDev.com, 1+858.375.2032.

Nomenclature

a	= Orbit Semi-major Axis
AIM	= Advanced Imagery Mechanism
C_3	= Square of the Residual Velocity at the boundary of gravitational Sphere of Influence (km^2/s^2)
D	= NEO Diameter
$DDT\&E$	= Design, Development, Test, and Evaluation
DSN	= Deep Space Network
e	= Orbit Eccentricity
FOM	= Figure of Merit
G	= Gravitational Constant ($6.6742 \times 10^{-11} \text{ N}\cdot\text{m}^2/\text{kg}^2$)
g_o	= Gravitational Acceleration at Earth's Surface (9.807 m/s^2)
h	= Height Above NEO Surface
i	= Orbit Inclination with respect to the Ecliptic Plane
Isp	= Rocket Engine Specific Impulse
JAT	= Java Astrodynamics Toolkit
LAD	= Laser Altimeter Device
LCC	= Life Cycle Cost
LEO	= Low Earth Orbit
m	= Spacecraft Mass
M	= NEO Mass
m_f	= Final Mass after Rocket Burn
m_L	= Rocket Delivered Payload Mass
m_o	= Initial Mass before Rocket Burn
m_p	= Rocket Propellant Mass
m_s	= Rocket Structural Mass
$NASA$	= National Aeronautics and Space Administration
NEO	= Near Earth Object
PTV	= Propulsive Transfer Vehicle
r	= NEO Radius
RCS	= Reaction Control System
$R\&D^3$	= Research and Development Degree of Difficulty
$ROSETTA$	= Reduced-Order Simulation for Evaluation of Technologies and Transportation Architectures
TFU	= Theoretical First Unit
TRL	= Technology Readiness Level
ΔV	= Delta-Velocity (m/s)
ε	= Structural Coefficient
μ_{sun}	= Gravitational Parameter of the Sun ($1.327 \times 10^{13} \text{ km}^3/\text{s}^2$)
ρ	= Magnitude of Position Vector in Heliocentric Orbit

I. Mission Overview

A. Introduction

The Foresight spacecraft is a concept design for a radio tagging mission to Near Earth Asteroid (NEO) Apophis. This NEO, officially referred to as 99942 Apophis (2004 MN4), has a probability of Earth impact of 2.2×10^{-5} (a 1 in 45,456 chance) on Friday, April 13, in the year 2036¹. In the year 2029 Apophis will approach the Earth to within xx km, closer than geostationary satellite orbits. If Apophis passes through a several-hundred-meter-wide "keyhole" in space during this approach, it will impact the Earth in 2036. If additional Earth-based observations are not sufficient to rule out an impact in 2036, a better determination of the object's orbit is required. Such precision may be obtained by "tagging" the object with a beacon, transponder or reflector on or near the asteroid. The Foresight spacecraft described here is a representative design for such an Apophis tagging mission and deemed useful as a starting point for future designs for potentially other hazardous objects.

Two, specific objectives of the Foresight spacecraft are as follows²:

- 1) Tracking from this mission should decrease the size of the 2029 error ellipse sufficiently fast so that if required, a deflection mission can be accomplished before the 2029 Apophis close encounter. For the purposes of this competition, data must facilitate a deflection mission decision by 2017 (enabling 3 years development for a deflection mission and 9 years to rendezvous and deflect).
- 2) Assume for this competition that the Apophis tracking accuracy must be adequate to reduce the long dimension of the $\pm 3\sigma$ error ellipse to 14 kilometers by 2017, the assumption being that such a level of confidence would be sufficient to prompt governments to launch a deflection mission. For reference, this translates approximately to a 10% impact probability if the keyhole is right in the middle of the 14-kilometer error ellipse.

The strategy employed by the Foresight mission for improving the knowledge of Apophis' orbital parameters is to send a small tracking spacecraft to Apophis to first determine its center of mass, and then track the asteroid of a period of time. Center of mass is determined using an on board Advanced Visual Imagery Mechanism (AIM) and Laser Altimeter Device (LAD) in conjunction with radio science through range measurements from the Deep Space Network (DSN). Once the center of mass has been determined, the spacecraft takes regular measurements of its position state relative to Apophis and maintains a constant separation from the asteroid's center of mass in a trailing heliocentric orbit. The DSN is used to accurately determine the range of the spacecraft from Earth over a period of time. These measurements are combined with an orbit determination algorithm to reduce the uncertainty in Apophis' orbital parameters until the long dimension of the $\pm 3\sigma$ of Apophis in 2029 is less than 14 kilometers.

The Foresight Encounter Spacecraft (ES) is similar in design to other Discovery class missions such as NEAR, Deep Impact, and Hayabusa as shown in Figure 1. Primary power is provided by two solar arrays, augmented by batteries. Communications are achieved with a combination of high and low gain antennas. The spacecraft is maneuvered by a single bi-propellant chemical main engine and a number of smaller thrusters using the same propellants. Flight proven equipment was selected for all of the major subsystem components. The scientific instruments are derived from similar missions. The spacecraft uses a Propulsive Transfer Vehicle (PTV), a simple bi-propellant chemical stage, to assist in achieving the necessary Earth departure velocity.

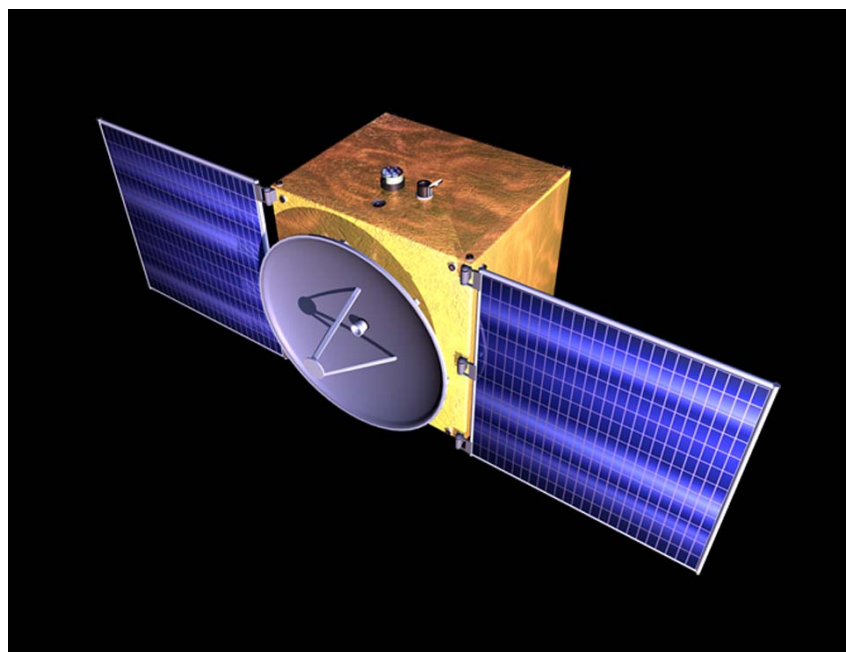


Figure 1. Foresight Encounter Spacecraft.

B. Overall Mission Summary

The overall concept of operations for the Foresight mission is shown in Figure 2.

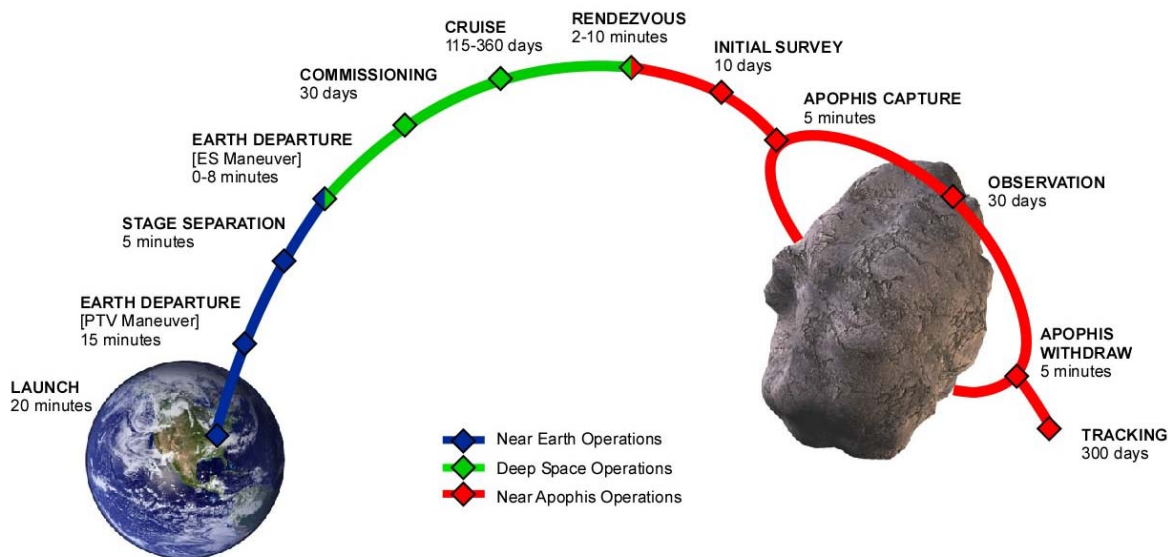


Figure 2. Foresight Concept of Operations and Mission Schedule for Target Launch Date.

The launch vehicle delivers the combined spacecraft and PTV to a 185.2 km by 185.2 km LEO. Upon delivery, the PTV immediately ignites its main engine and initiates the Earth Departure [PTV Maneuver] phase. The main engine on the PTV fires for roughly 15 minutes. Once this maneuver is complete, pyrotechnic staging is used to separate the spacecraft from the PTV. For some launch windows, to achieve the necessary departure delta-V the spacecraft required to perform the Earth Departure [ES Maneuver]. A successful Earth Departure maneuver places the spacecraft on a transfer orbit from Earth to Apophis, and the mission enters the Cruise phase. The first 30 days of cruise are used for a Commissioning phase. During this period, various functional routines are performed and telemetry is analyzed to assure all subsystems are functioning nominally. The spacecraft's solar arrays are also deployed and activated, charging the batteries and providing power to the bus during this phase. Pre-arrival tests of the Guidance, Navigation, and Control (GNC) systems are performed. The scientific instruments are activated and tested. The Cruise can last from 115 to 360 days depending on the launch opportunity. During this period, spacecraft subsystems are monitored and regularly tested to ensure proper functionality. The spacecraft is oriented with its solar arrays facing the Sun and draws all of its necessary power from the arrays.

When Apophis comes in range of the the AIM, the spacecraft's main camera, the camera is used to track the asteroid and, in conjunction with the RCS thrusters, perform trajectory refinement maneuvers to ensure that the spacecraft will intercept Apophis. At a range between 200 km and 1,000 km depending on the launch opportunity, the spacecraft activates its main engine to begin the Trailing Capture Maneuver. This maneuver can take from 2-10 minutes, again depending on the launch opportunity. After completion of the the Trailing Capture Maneuver, the spacecraft is positioned to a separation distance of 10 km from Apophis, in a heliocentric orbit match with Apophis (leading or training depending on the opportunity). At this point, an Initial Survey is taken of the asteroid, lasting up to 10 days. The scientific instruments are tested, and the high gain antenna is activated to transfer the first close-up images of Apophis back to Earth.

Once proper functionality of all instruments and subsystems has been confirmed, the spacecraft performs the Apophis capture maneuver and enters into an orbit about Apophis, beginning the Observation phase. The goal of the Observation phase is to generate accurate mass, bulk density, gravitational, and shape models of the asteroid. These models are generated in a similar fashion to those of Eros by the NEAR mission using a 30 day data arc combining laser rangefinder and imager data³. During this phase, the spacecraft maintains an orientation with the solar arrays facing the Sun and the scientific instruments facing Apophis so as to facilitate continuous fully powered data

acquisition. Major data downlinks to the DSN occur once per week: during these periods, the spacecraft is rotated to aim the high gain antenna at the Earth and the batteries augment the non-optimal solar array power production.

At the end of the Observation phase, the spacecraft withdraws from the Apophis orbit and enters an Apophis-trailing heliocentric orbit with a 2 km separation from the asteroid. This marks the beginning of the major phase of asteroid proximity operations, the Tracking phase. During this entire phase, the spacecraft maintains its 2 km separation from Apophis in the trailing heliocentric orbit. Figure 3 shows a diagram of relative locations of the spacecraft, Apophis, the Earth, and the Sun during this phase. Due to the geometry of the problem and Apophis' relatively low orbit eccentricity, from a position of 2 km behind Apophis, the spacecraft is able to maintain an orientation such that the laser rangefinder and imager are facing the asteroid while the Sun is at nearly 0° to the solar arrays. As seen on Figure 3, the position of the Earth varies significantly during this phase but is always on the side of the spacecraft facing the Sun.

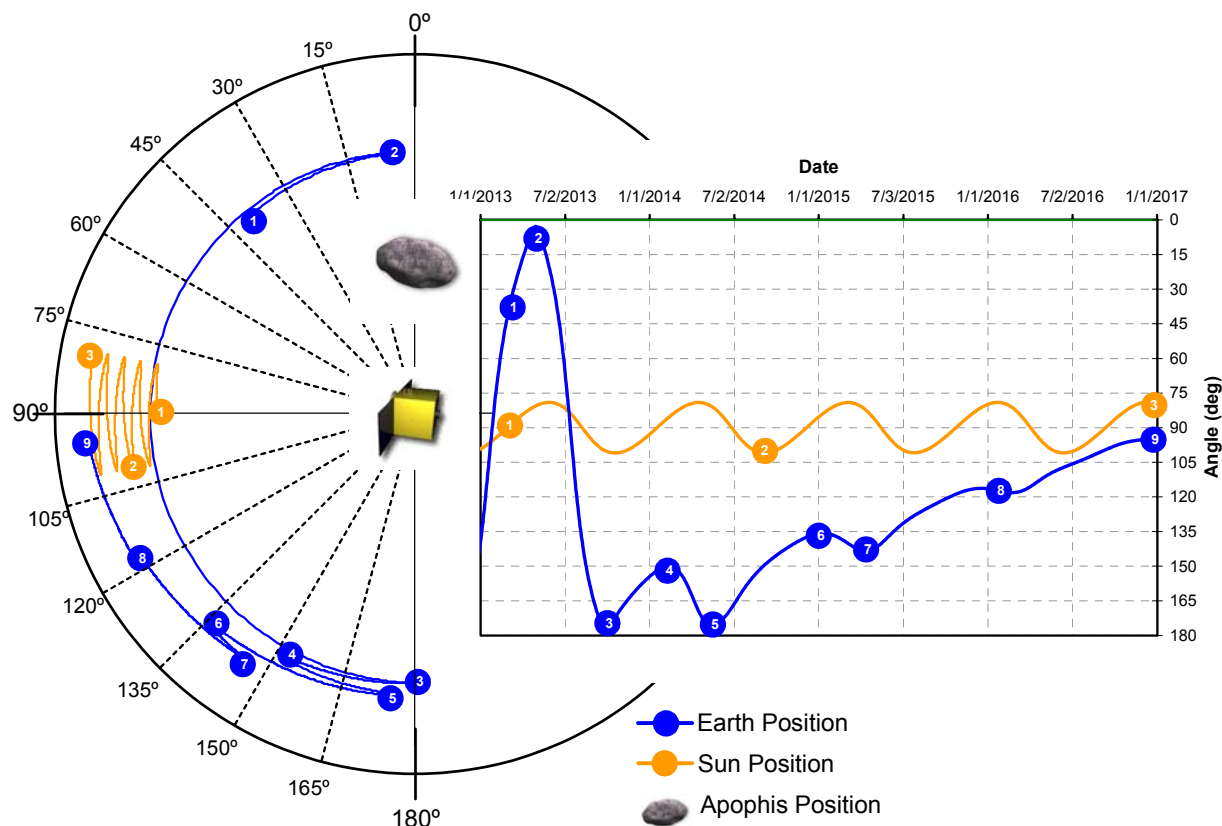


Figure 3. Sun Earth Angles

During the Tracking phase, the spacecraft measures its position from the asteroid and maintains a 2 km separation from Apophis' center of mass. The position of the spacecraft is measured once a week by the DSN while the spacecraft transmits its range vector from the asteroid. Station-keeping is required to counteract the perturbing forces of the other major gravitational bodies in the solar system. After 300 days of these weekly measurements, the orbit of Apophis will have been determined to sufficient accuracy to meet mission requirements. At this point, depending on the amount of equipment lifetime and vehicle propellant remaining, an Extended Mission phase could be entered to further reduce the uncertainty of Apophis' orbit.

The full range of launch windows offers 134 days worth of launch opportunities spanning nearly two and a half years. The target launch date for this mission represents the optimal launch opportunity in the primary launch window and corresponds to the mission scenario in which the PTV is capable of performing the entire Earth departure maneuver without assistance from the ES. The timeline for the target launch date of May 9, 2012 is outlined in Table 1. The transfer trajectory yields a transfer time of 310 days from Earth to Apophis. At Apophis interception, the spacecraft has greater orbital energy than the asteroid and therefore uses its Trailing Capture Maneuver to reduce its orbital energy and enter in an Apophis-trailing heliocentric orbit for the Initial Survey

period. Assuming the complete use of the 10 day Initial Survey period and 30 day Observation period, this opportunity yields a 650 day, or roughly 22 month, mission from launch to mission completion.

Table 1. Timeline for Primary Launch Date

No.	Mission Phase	Date (initial)	Duration	Mission Time (dd:hh:mm)
1.	Launch	5/9/2012	20 minutes	T = 0:00:00
2.	Earth Departure: PTV Maneuver	5/9/2012	15 minutes	T = 0:00:20
3.	Stage Separation	5/9/2012	5 minutes	T = 0:00:35
4.	Commissioning	5/9/2012	30 days	T = 0:00:40
5.	Cruise	6/8/2012	310 days	T = 30:00:00
6.	Trailing Capture Maneuver	3/15/2013	10 minutes	T = 310:00:00
7.	Initial Survey	3/15/2013	10 days	T = 310:00:10
8.	Apophis Capture Maneuver	3/25/2013	5 minutes	T = 320:00:00
9.	Observation	3/25/2013	30 days	T = 320:00:05
10.	Apophis Withdraw Maneuver	4/24/2013	5 minutes	T = 350:00:00
11.	Tracking	4/24/2013	300 days	T = 350:00:05
12.	Extended Mission	2/18/2014	x	T = 650:00:00

C. Launch Opportunities

1. Interplanetary Trajectory Analysis

In order to determine mission launch opportunities, a sweep of potential Earth-Apophis transfer trajectories was performed using Bullseye, a Java-based trajectory analysis software package developed internally at SEI. Bullseye combines ephemeris data and a Lambert's problem solver to determine the interplanetary trajectory between two Solar System bodies for a given time of flight. Ranges on desired departure and arrival dates are available inputs to the simulation. Bullseye calculates the transfer orbit between the two bodies for each unique combination of departure and arrival dates and outputs the arrival and departure C3 values for each combination.

To allow for sufficient time for spacecraft development and testing, the earliest potential departure date for this mission was constrained to be 1/1/2011. The mission parameters dictate that all observation and tracking should be complete by 1/1/2017, and a minimum operations time of roughly one year is required for asteroid mass modeling and orbit determination, so the latest potential arrival date for the mission is constrained to be 1/1/2016. A sweep of Earth-Apophis transfer trajectories between 1/1/2011 and 1/1/2016 was performed in Bullseye to determine potential launch opportunities for this mission. Once this sweep was complete, the data was post-processed. Required delta-Vs from a 185.2 km by 185.2 km LEO to the edge of Apophis' sphere of influence were calculated and the minimum total delta-V trajectory for each departure date in the window was determined. The departure, arrival, and total delta-V for these solutions are presented in Figure 4.

From preliminary spacecraft modeling and mass estimation, it was determined that a total delta-V limit of 6,000 m/s represented an ideal compromise between spacecraft size and launch flexibility. With a limit of 6,000 m/s, five individual launch windows were identified as seen in Figure 4. Launch windows 1 and 3 represent fairly deep launch opportunities in terms of total delta-V and were therefore selected as the primary and secondary launch windows due to their performance advantage. Though window 3 offers the best performance, window 1 was selected as the primary because it offers the earliest launch opportunities. Launch windows 2, 4, and 5 serve as alternate windows should the primary and secondary be unusable.

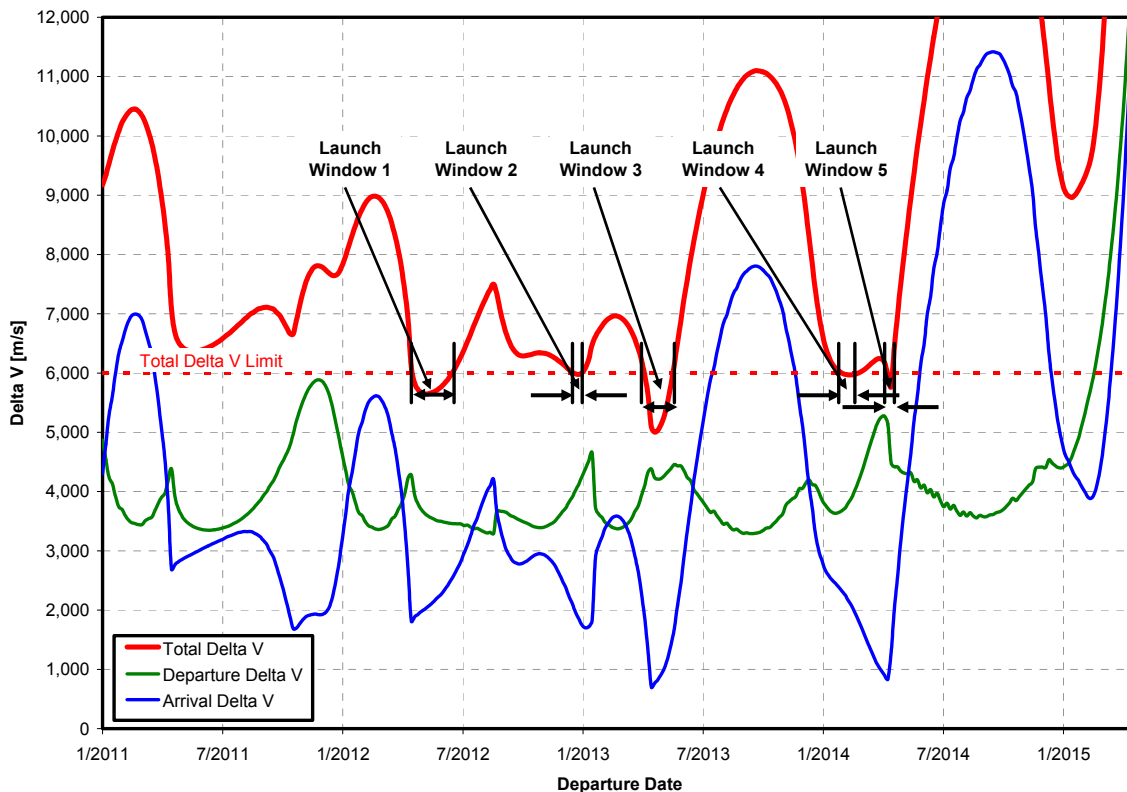


Figure 4. Departure, Arrival, and Total Delta-V for Minimum Total Delta-V Trajectories from LEO to Apophis.

2. Launch Window Analysis

Analysis of the five available launch windows showed that the division of delta-V between Earth departure and Apophis arrival was significantly different across the launch windows. It was therefore decided that the spacecraft would be sized to perform the maximum Apophis arrival delta-V necessary, and would also be used to augment the PTV in performing the Earth departure maneuver. The spacecraft would therefore be capable of providing all of the arrival delta-V necessary without assistance from the PTV, while the PTV would not need to be oversized to provide all of the necessary departure delta-V. The arrival delta-V limit of these five launch windows was set be 2,400 m/s based on preliminary vehicle mass estimates: this limit is displayed on Figure 5, along with the vehicle total delta-V limit of 6,000 m/s determined earlier. It should be noted that the primary launch window is limited in its end date by the arrival delta-V limit rather than the total delta-V limit; all other launch windows are limited by the total delta-V limit.

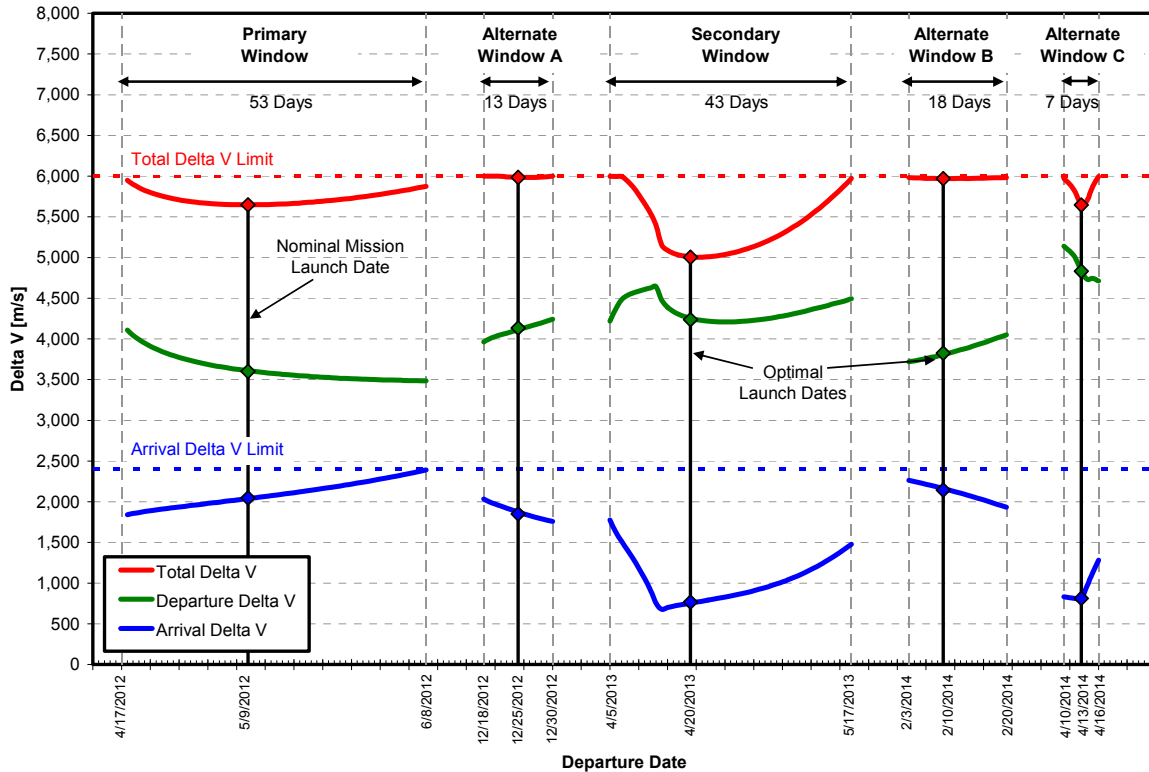


Figure 5. Departure, Arrival, and Total Delta-V for Minimum Total Delta-V Trajectories from LEO to Apophis for Specified Launch Windows.

The start and end dates for each launch window are shown in Figure 5, as well as the optimal launch date for each window. The optimal launch date represents the lowest total delta-V opportunity within each window. In the case of the primary launch window, this launch date also represents the point at which the departure delta-V is exactly 3,600 m/s, meaning the PTV can perform the entire Earth departure maneuver without assistance from the spacecraft itself.

The arrival dates corresponding to the selected launch windows are shown in Figure 6. The latest arrival date possible is 1/28/2015. Arriving at this date would allow 704 days of operation before the 1/1/2017, the latest possible date for mission completion. This is well within the mission requirement of one year at Apophis.

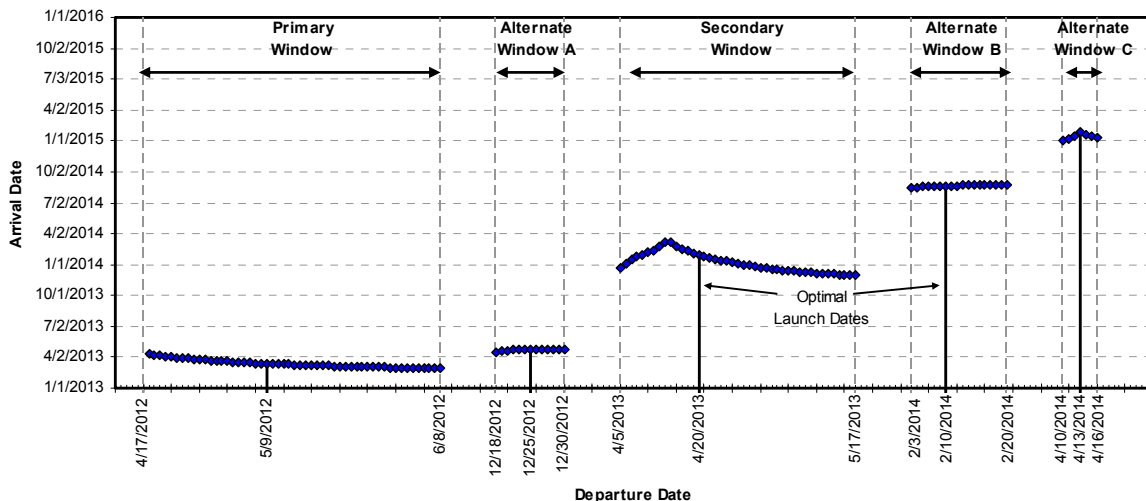


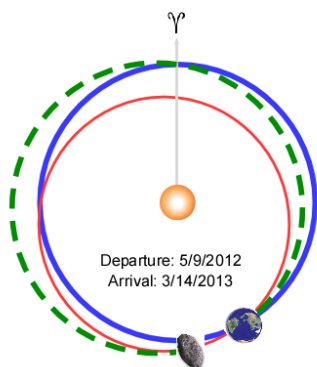
Figure 6. Arrival Dates for Launch Window Trajectories.

The transfer trajectories corresponding to the minimum total delta-V solution within each launch window are presented in Figure 7. These graphics were generated using Bullseye. Their corresponding parameters are displayed in Table 2.

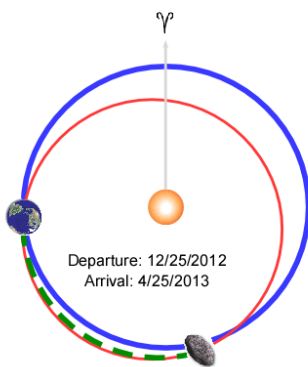
Table 2. Minimum Total Delta-V Earth-Apophis Transfer Trajectories for each Launch Window

Mission Phase Information	Primary	Alternate A	Secondary	Alternate B	Alternate C
Earth Departure					
Departure Date	5/9/2012	12/25/2012	4/20/2013	2/10/2014	4/13/2014
Departure C3 [km ² /s ²]	8.3074	20.7668	23.2841	13.5017	37.9047
Departure Delta V [km/s]	3.5986	4.133	4.238	3.8244	4.831
Transfer Orbit					
Semi-Major Axis [AU]	1.032	0.930	0.957	0.844	0.879
Eccentricity	0.076	0.156	0.146	0.181	0.222
Inclination [deg]	2.398	0.434	3.048	1.627	3.730
Long. Ascending Node [deg]	229.062	273.702	210.371	141.514	203.278
Argument of Periapsis [deg]	77.615	60.571	117.604	162.595	138.530
Departure True Anomaly [deg]	282.415	119.652	242.413	197.364	221.481
Arrival True Anomaly [deg]	216.790	222.872	190.409	108.967	211.849
Apophis Arrival					
Arrival Date	3/15/2013	4/25/2013	1/26/2014	8/21/2014	1/28/2015
Arrival C3 [km ² /s ²]	4.1942	3.4271	0.5867	4.5954	0.6625
Arrival Delta V [[km/s]	2.0479	1.8512	0.7659	2.1437	0.8139
Totals					
Total Delta V [km/2]	5.6466	5.9842	5.0039	5.9681	5.645
Total C3 [km ² /s ²]	12.5015	24.1938	23.8708	18.0972	38.5672
Total C3 [km ² /s ²]	12.5015	24.1938	23.8708	18.0972	38.5672

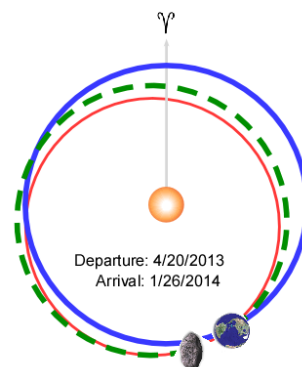
Primary Launch Opportunity



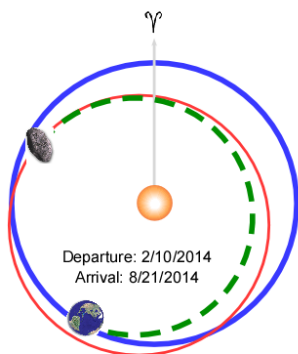
Alternate Opportunity A



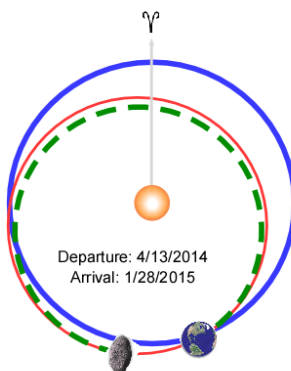
Secondary Launch Opportunity



Alternate Opportunity B



Alternate Opportunity C



- Earth Orbit ——— Blue
- Apophis Orbit ——— Red
- Transfer Orbit ——— Dashed Green
- Earth Position at Departure — Earth icon
- Apophis Position at Arrival — Apophis icon

Produced Using SEI's *Bullseye* Trajectory Analysis Tool



Figure 7. Minimum Total Delta-V Earth-Apophis Transfer Trajectories for each Launch Window

3. Delta-V Budgets

The delta-V budgets for the PTV and spacecraft for each optimal launch opportunity within the launch windows are outlined in Figure 8. In addition to the 3,600 m/s delta-V capability of the PTV, an additional 2.5% (90 m/s) of reserves was added to this vehicle to represent unused residual propellant at the end of the burn. Reserves for the spacecraft are determined based on remaining delta-V for each launch opportunity; the reserves encompass all of the propellant not expended for the two transfer maneuvers and not allocated for maneuvering or station-keeping. The division of the Earth departure and Apophis arrival burn by the spacecraft is shown for each opportunity. For the primary launch opportunity, the spacecraft is not required to burn for the Earth departure maneuver.

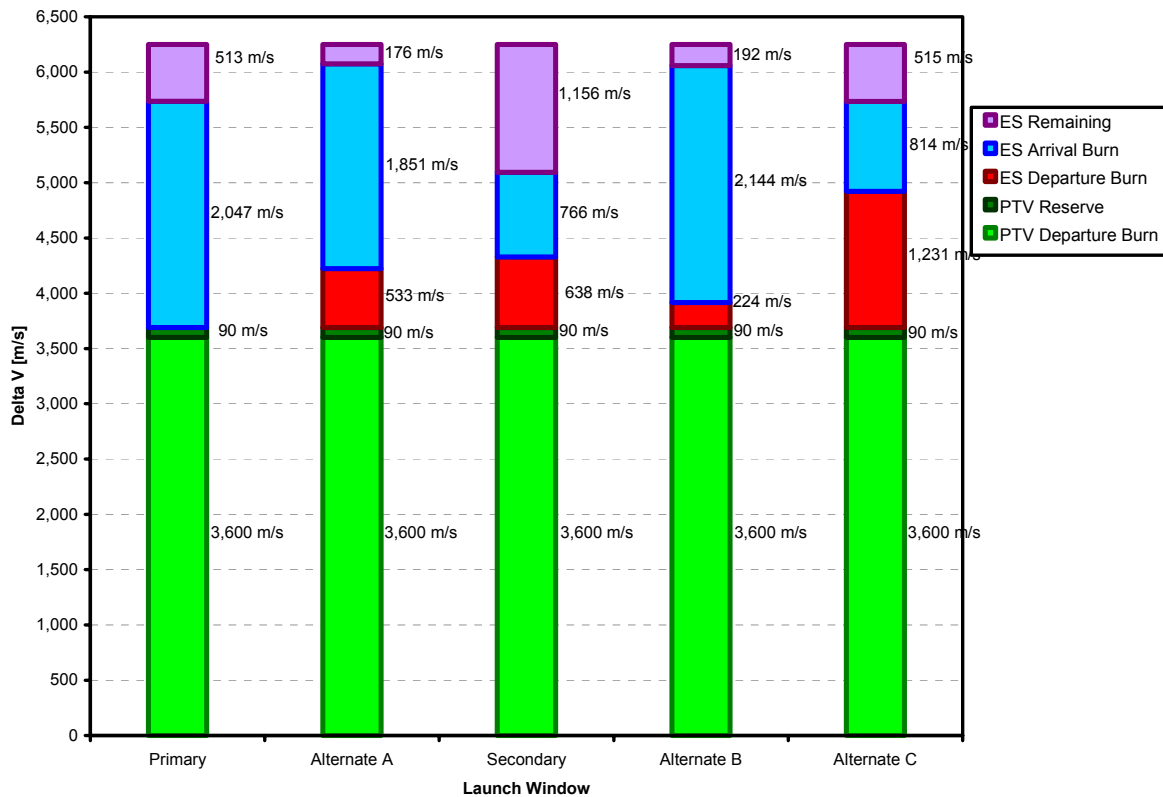


Figure 8. Spacecraft and Propulsive Transfer Vehicle (PTV) Delta-V Budget for Optimum Launch Dates within each Launch Window.

The propellant remaining in spacecraft after the Apophis arrival maneuvers are complete is divided between station-keeping, maneuvering, and reserves: a detailed delta-V budget for the spacecraft is presented in Figure 9. Station-keeping is required to counteract the perturbing accelerations from the other gravitational bodies in the solar system. Jupiter presents the largest perturbing force, with Earth and Venus as secondary perturbing forces; the other bodies in the solar system provide only a negligible perturbation over the duration of the mission. Once the spacecraft has entered the tracking phase of the mission and is outside of Apophis' sphere of influence, Apophis becomes the dominant perturbing force in the gravitational model. A station-keeping budget of 20 m/s per year was calculated based on the average perturbing accelerations from these local bodies. To be conservative, the ES carries three years of station-keeping delta-V, or 60 m/s. In addition to countering perturbing forces, the ES must also perform a number of maneuvers around Apophis during the observation phase of the mission in order to maintain, correct, and modify its orbit about the asteroid.

The propellant remaining after the departure, arrival, station-keeping, and maneuvering budgets is considered reserve. This propellant is available to support an extended mission once the primary mission objectives have been successfully met.

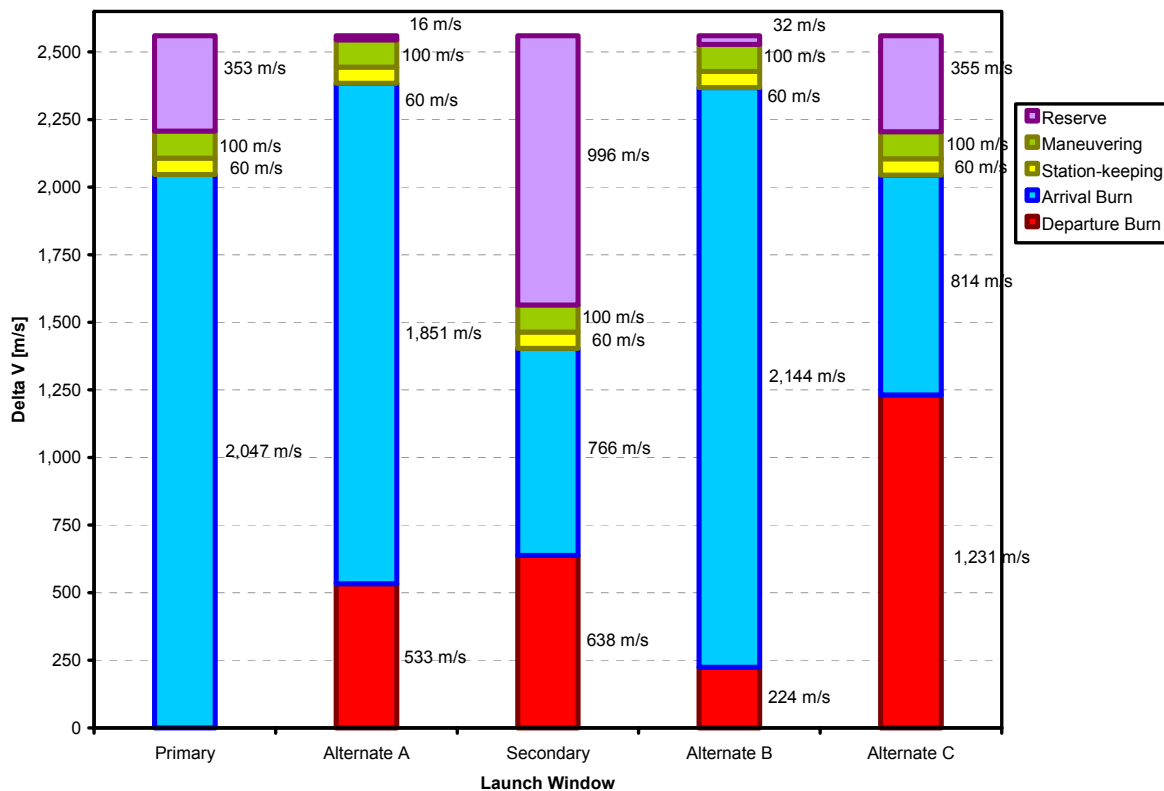


Figure 9. Spacecraft Delta-V Budget for Optimum Launch Dates within each Launch Window.

D. Launch Vehicle Selection

The Orbital Sciences Corporation (Orbital) Minotaur IV launch vehicle was selected as the primary launch vehicle for the Foresight mission. The Minotaur IV provides medium payload delivery to LEO at a competitive price and relatively quick (18 month) mission response time including payload integration and launch. The combination of a Minotaur IV and a PTV gives significant cost savings as compared to a larger interplanetary launch vehicle with no PTV. The Minotaur IV consists of three Peacekeeper solid rocket stages and a commercial Orion 28 fourth stage. Its avionics and support subsystems are heritage technologies from Orbital's Pegasus, Taurus, and Minotaur launch vehicles. The Minotaur IV is scheduled to begin service in December, 2008 and will be available during the launch period required of this mission to launch U.S. government-funded payloads⁴.

The Foresight spacecraft will launch from Pad 0B at the Mid-Atlantic Regional Spaceport (MARS) facility located at the Wallops Flight Facility in Virginia. The MARS has been host to several successful Minotaur launches and serves as Orbital's primary launch location for low inclination Low Earth Orbit (LEO) payloads. The Minotaur IV will deliver the combined Foresight spacecraft to a 185.2 km (100 nm) circular LEO⁵.

The payload performance to LEO of the Minotaur IV is shown in Figure 10. Because the performance (specific impulse) of the Minotaur IV upper stages is lower than that of the bipropellant engines chosen for the Foresight vehicles, it was decided to size the Foresight vehicle to the 1,680 kg maximum deliverable payload to LEO by the Minotaur IV from the MARS. This allows the Foresight vehicle to perform the majority of the Earth departure maneuver itself thereby increasing the deliverable payload to Apophis. To further maximize performance, the Foresight vehicle will be launched on a due east trajectory from the launch site, i.e. into a 38° inclination departure orbit.

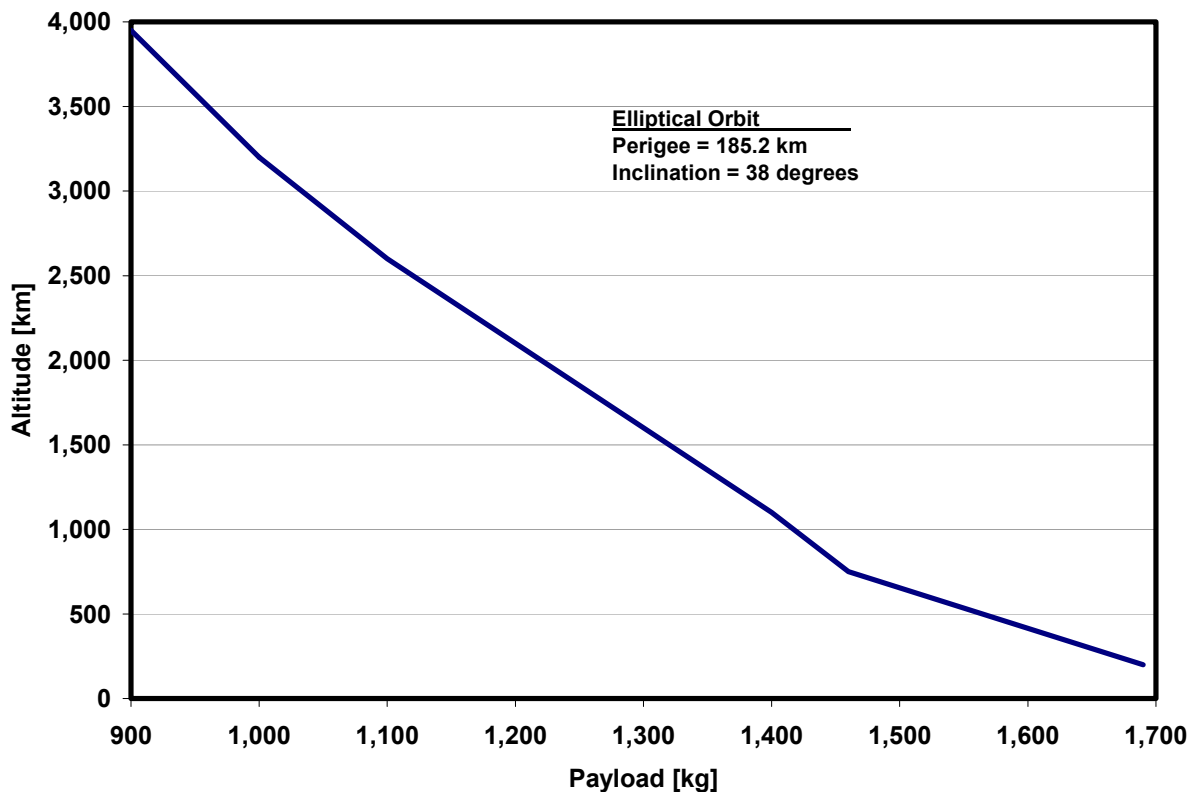


Figure 10. Minotaur IV Payload Performance to LEO at various LEO Apogee Altitudes⁵.

Should the Minotaur IV be unavailable or determined to be unsuitable for this mission, the Lockheed Martin Athena II can serve as an alternative launch vehicle. The Athena II lifts 2,065 kg payload to a 200 km LEO, sufficient to carry the Foresight vehicle with 22% margin. The Athena II launches from the Cape Canaveral Air Force Station launch site and delivers its payloads to a 28.5° inclination orbit with a due east launch⁶. Should a non-US launch vehicle be preferred, the Rockot, a Russian launch operated by Eurockot Launch Services, can deliver 1,950 kg to a 200 km LEO at 63° inclination⁷.

II. Apophis Orbit Determination and 2029 Error Ellipse Prediction

A. Introduction

The objective of this mission is to conduct precise in-situ measurements of the position of Apophis in order to enable a very accurate determination of the NEO’s heliocentric orbit. According to S. R. Chesley in 2005, the 2029 Apophis-Earth encounter distance is predicted to be 5.89 Earth radii, ± 0.35 Earth radii, (3σ) based on current knowledge⁸. This equates to an approximate largest dimension of the 3σ error ellipse of 4500 km. Our goal is to determine the orbital state with sufficient precision, so that when it is propagated forward to the close approach with Earth in 2029, the long dimension of the $\pm 3\sigma$ error is reduced to less than 14 km (i.e. 6 times sigma). Per the rules of the Planetary Society Apophis Mission Design Competition, this objective must be met by 1/1/2017. Our measurement approach is two-fold:

- 1) Accurately determine the location of the center of mass of Apophis relative to the Foresight spacecraft.
- 2) Accurately determine the position of the Foresight spacecraft relative to the Earth and Sun.

B. Locating the Center of Mass of the Target Asteroid

Reduction of the error ellipse of Apophis first requires the ability to precisely measure the position of Apophis’ center of mass with respect to the Foresight spacecraft. Before these measurements can be made, an accurate shape, rotation, and gravitational model of the asteroid must be developed. These models will be generated during the Observation phase of operations using the PCODP software tool developed by J. K. Miller, et al and used during the

Near-Earth Asteroid Rendezvous (NEAR) mission to generate similar models for the asteroid Eros³. Optical tracking of landmarks from imaging data generated by the onboard camera along with range data generated by the laser altimeter are used to generate an accurate shape (topography) model and determine rotational details of the asteroid. These data are also used to accurately determine the spacecraft's position with respect to the asteroid's volumetric centroid. While the spacecraft is in orbit about Apophis, continuous prediction of the spacecraft's position with respect to the surface features is combined with the Deep Space Network (DSN) measurements of the spacecraft's position and the spacecraft's own measurements of its position with respect to Apophis to generate a detailed model of Apophis' gravitational field. These three models can then be joined to determine the center of gravity and associated gravity potential parameters. Our assumption is that this process, already established during the NEAR mission, can be relied upon to produce highly accurate measurements from the Foresight spacecraft to Apophis' center of gravity and its center of mass.

C. Locating Foresight with Respect to the Earth

Once the center of mass and spin axis of the asteroid have been determined, the spacecraft enters the Tracking phase of the mission. From a trailing heliocentric orbit, a series of range measurements from the asteroid to the spacecraft are used in conjunction with the DSN to predict the range from the Earth to the Foresight spacecraft. While DSN can provide reasonably accurate measurements of deep space spacecraft position and velocity, its accuracy based on a single measurement or two is insufficient to determine the orbital parameters to the precision required for this mission. Our analysis indicates that at a given epoch on the 2017 timeframe, the position and velocity of Foresight (and therefore Apophis' center of gravity) *must be known to within tens of meters and thousandths of a millimeter per second in velocity* in order to reduce the error ellipse in 2029 to the required accuracy.

A single DSN measurement has 1σ accuracies of roughly 2 meters in the range direction (quite good), but around 2.5 nanoradians in transverse sweep angle⁹. At 1 AU, this transverse sweep angle inaccuracy corresponds to a transverse position inaccuracy on the order of kilometers, orders of magnitude larger than the range inaccuracy. Spacecraft velocity is often estimated over two DSN measurements, differencing position over the time between the measurements. This technique results in velocity accuracies on the order of millimeters per second, but does not produce the velocity accuracies necessary to solve the present problem. The use of two DSN ground stations (the so-called Delta-DORS or Delta Doppler range observation technique) is likewise insufficient to provide the necessary accuracies with a single measurement or two.

Our approach is to conduct a series of measurements over a long time arc (many days) in order to produce the necessary accuracy. Since range is the most accurate measurement available from the DSN, our technique only relies on the use of range information (distance along the sight line). A series of range measurements can be used as the basis of a batch filter algorithm (like a one-time Kalman filter) to accurately predict the orbital state at beginning of the measurement arc. The following sections outline our approach toward modeling the orbital mechanics and establishing both the required frequency of DSN range measurements and the duration of the measurement arc.

D. Approach to Error Ellipse Reduction

1. Orbit Propagation and Error Ellipse Estimation

In order to model this problem, internal software tools were developed by the Foresight team to accurately propagate Apophis's orbit state and predict the uncertainty in Apophis' state as a function of number of measurements and time between measurements. An 8th/9th order n-body numerical propagator with a variable step size was used to propagate the actual and dispersed orbits of Apophis forward from a given state and epoch. The sun, all of the planets and the Earth's moon are considered in the gravitational model. The perturbing effects of the large asteroid-belt asteroids Ceres, Pallas, and Vesta are also included. Solar pressure and the Yarkovsky effect are not modeled, but their associated uncertainties are addressed in the analysis. For a given starting condition, the propagator's step-wise integration tolerances were set so that results for position accuracies were on the order of a few meters in 2029.

For the time period considered, Apophis' orbit must be propagated from a starting state for approximately 12 years. This period includes a relatively close approach to Earth in 2021. The propagation eventually reaches the particular close approach in April of 2029 that might result in Apophis passing through a "keyhole" on the b-plane that will change its orbit to a 7:6 resonant return and impact in 2036. The accuracy of this numerical propagator was verified against published data and similar sample cases.

Acknowledging the detrimental perturbation effects of solar pressure and the Yarkovsky effect, we nonetheless consider that the largest uncertainties on eventual location of the asteroid in 2029 are due to the uncertainty in its

state at the start of the Tracking phase of our mission. Our simulation determines the future error ellipse from the initial state errors by direct propagation. For our detailed investigations, we typically run 1000 Monte Carlo simulations sampled from the initial normal state position and velocity error distributions to determine the shape and nature of the error ellipse in 2029. These simulations were run on a fast Windows-class PC with a 2 GHz Pentium processor. A single job of 1000 Monte Carlo simulations typically takes 8 – 10 hours to complete.

NEO fly-by and keyhole analyses are most clearly and conveniently portrayed in the two-dimensional b-plane. This planetocentric plane is explained in detail by Valsecchi¹⁰. For our problem, the b-plane is centered on the Earth and is normal to the incoming asymptote of the approaching asteroid in April of 2029. Therefore for this analysis, our discussions of the “error ellipse” are assumed to be dimensions in the 2D b-plane rather than a larger 3D error ellipse “cloud” that would physically exist and be viewed by a remote observer as a long distribution of potential locations of Apophis along its heliocentric orbit at a given time. It is worth noting that for this particular fly-by encounter, the longest dimension of the 2029 error ellipse in 3D space is nearly identical to that of the error ellipse projected in the b-plane since the approach angle is shallow and the velocities of the Earth and Apophis are relatively similar, so either method would provide similar values.

2. Orbit Determination Method

As previously discussed, we propose to use a batch filtering method to process the series of range measurements that will be collected by Foresight and use them to predict a highly accurate initial orbital state. To establish that this technique will work for the proposed collection frequency and measurement arc length, we developed a “proof-of-concept” implementation. This proof-of-concept implementation has also been used to help establish our overall mission concept of operations.

When Foresight arrives at Apophis, we assume that the asteroid has some exact reference state. This exact state is, of course, unknown to the spacecraft and ground observers. For proof-of-concept simulation purposes, we assume that this reference state on 1/1/2015 is the mean orbital state predicted by the JPL *Horizons* computer system for that date. *Horizons* is JPL’s on-line ephemeris system, which includes high accuracy ephemerides for over 170,000 celestial bodies including Apophis¹¹. We recognize that additional optical and radar observations of Apophis between now and 2015 will affect that prediction, but that fact will not affect the viability of the proposed approach. Note that our approach does not assume the addition of new ground observation data during the measurement arc or during the subsequent 12-year propagation to 2029, so it is therefore somewhat conservative.

To test our batch filter approach and gain confidence that it will work for a actual flight mission, we create a set of sample data by propagating the reference state forward in time. At appropriate times corresponding to DSN measurement locations, we calculate the range from Foresight to Earth. To this range measurement, we add a DSN range measurement error (+/- 2m, 1σ normal distribution). This perturbed range becomes the range value input to the filter (ρ_{meas}). The propagation is advanced to the next measurement time and a new range and range error are calculated. In this manner, we populate a vector of “measured” ranges over the arc. A measurement frequency of one week and an arc length of one Earth year would therefore result in 52 measured ranges. We utilize all gathered measurements simultaneously in order to generate a prediction of the initial orbit. This method is analogous to applying a curve fit through the measurements in order to predict the orbit.

An optimizer is given control over the six elements of asteroid’s state at the beginning of the arc and solves for those values of initial position and velocity that result in the best least squares fit of the measured ranges. The optimizer’s objective function is presented as Equation 1.

$$f = \sum_{i=1}^n [(\rho_{i_g} - \rho_{i_meas})^2] \quad (1)$$

Here, ρ_{i_meas} are the measured ranges (created from the reference state discussed above), and ρ_{i_g} are the predicted ranges associated with the optimizer’s predicted or “guessed” trajectory at each measurement location. The predicted range values correspond to the propagation of the initial state which the optimizer is varying. n is the number of range measurements taken over the time arc. The optimizer is deemed to have converged on the best initial state when the average range error falls within a 4 m tolerance across all of values in the vector. This process is described in Figure 11.

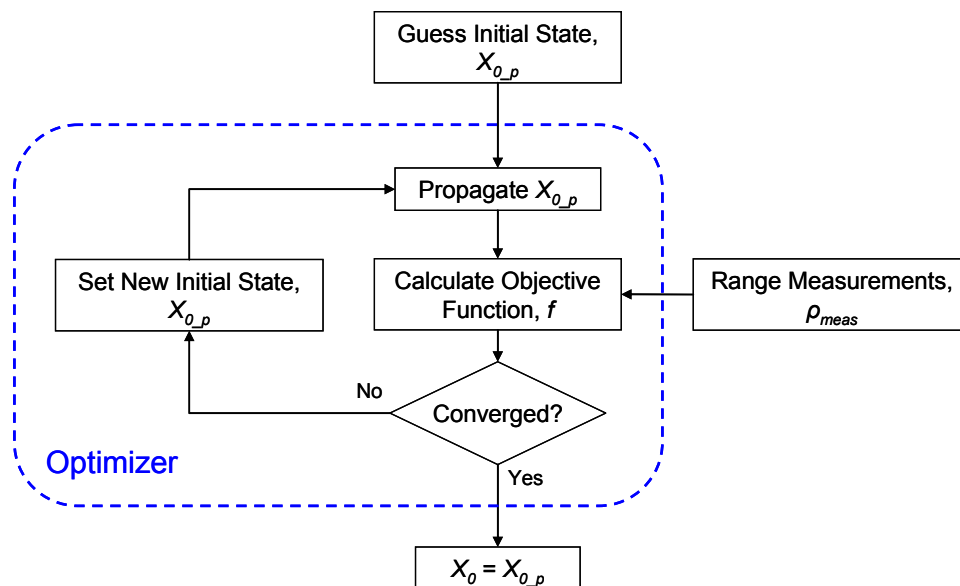


Figure 11. Batch Filter Algorithm

The optimizer is presented with an initial guess for the state of the orbit when the measurements begin, X_0 . The optimizer iterates on the prediction of the state, $X_{0,p}$, until the objective function, f , has reached convergence. Once optimized, this initial state is propagated forward from the start of the Tracking phase to April 2029 and represents a single possible point on the target b-plane. To establish the distribution of candidate points on the b-plane, we repeat this process many times with a new initial guess, a new set of measurement errors, and therefore a new predicted state from the optimizer.

3. Orbit Determination Optimizer

The process above was found to be sensitive to the optimization algorithm selected for the task and the initial guess it was provided with for X_0 . Gradient-based solvers were found to have difficulty establishing reliable derivatives, so we utilized non-gradient (zero-order) methods. In this regard, Powell's Method was found to be superior to the simpler Coordinate Pattern Search approach. Powell's Method is a univariate technique that builds a gradient-like conjugate search direction in order to increase its convergence speed¹². The initial guess for the starting state was found to be an extremely important parameter in reliable optimization of the batch filter. We assumed that for the actual mission, the state of Apophis would be reasonably well known and could be used as a starting point in the batch filter process. To model this effect in our proof-of-concept, we provided the optimizer with a random initial guess based on the reference orbital state plus position and velocity errors corresponding to values that could be determined from single DSN measurements (taken as normal distributions for sample purposes). For initial guesses, a DSN measurement was assumed to have a one-sigma position error of approximately 0.5 km and one-sigma velocity error of 5 mm/s, where the velocity error was calculated through a Gauss solver using two successive measurements.

E. Measurement Frequency and Arc Length Trades

In order to determine the necessary measurement arc length duration and measurement frequency to accomplish the desired goal of reducing the largest dimension of the 2029 error ellipse to 14 km ($\pm 3\sigma$) the batch filter algorithm was run repeatedly with various candidate measurement durations and frequencies. The optimizer was run for measurement durations between one month and two years. The measurement frequency was varied from one measurement every two days, to one measurement every two weeks.

For each measurement frequency and duration combination, a Monte Carlo analysis was performed with a random initial state guess detailed above, along with randomly perturbed range measurements. For each case, the converged (optimized) initial state was then propagated forward to the 2029 close approach. The cases were then projected on to the b-plane, forming the 2029 error ellipse of interest. Standard deviations could be calculated from the dispersions, and the largest standard deviation was determined for each of the measurement frequency and duration combinations.

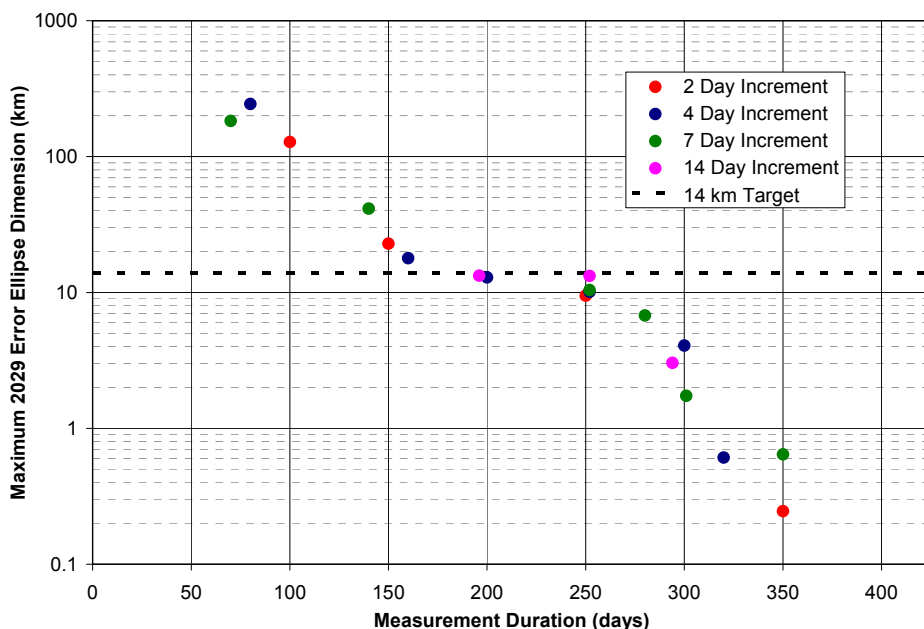


Figure 12. Range Measurement Regimen Comparison

Figure 12 depicts the approximate 2029 error +/- three-sigma error ellipse largest dimension for the various measurement frequency and duration combinations analyzed. As expected, increasing measurement duration decreases the orbit determination uncertainty upon the conclusion of measurements, which translates to a decrease in uncertainty in 2029. For a given frequency of measurement, longer measurement durations essentially result in more measurements. Note that varying the measurement frequency does not drastically affect the accuracy relative to modification of the duration. It appears that a large arc length (advance of Apophis around the sun) is the primary factor in determining an accurate orbit. Also, the error ellipse size is observed to drop significantly after a full Apophis orbit period, around 320 days. Measurements taken after a full Apophis orbit do not create much improvement, since they become somewhat redundant with the early measurements.

F. Selected Measurement Frequency and Duration

Based on our simulations, we propose to baseline a weekly measurement frequency for a period of 300 days (approximately 43 DSN range measurements). This solution represents a reasonable compromise between orbit determination accuracy, mission cost, and operational complexity. The error ellipse reduction vs. time for the selected parameters is shown in Figure 13.

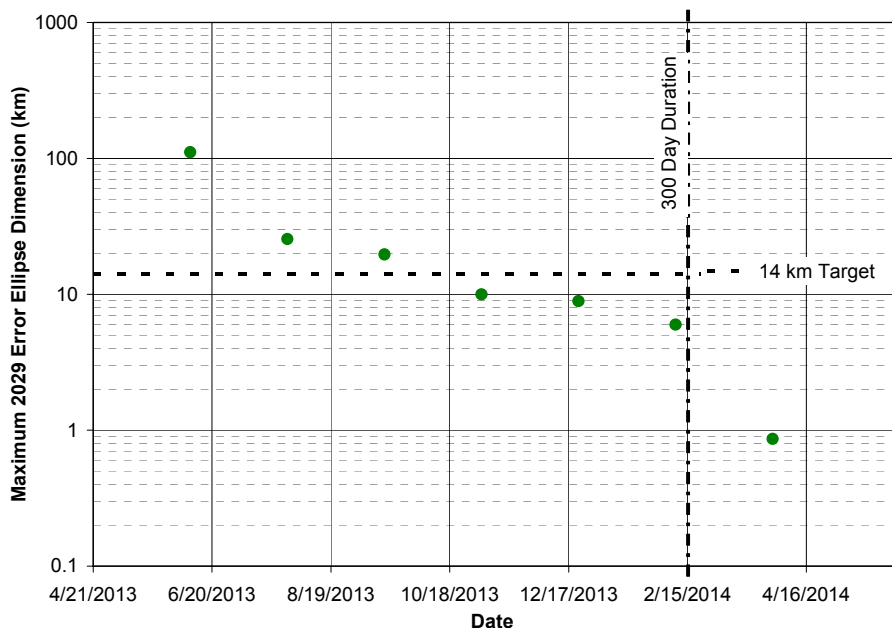


Figure 13. Error Ellipse Reduction for Target Mission

After taking measurements for 300 days, the error ellipse is reduced to under 6 km, ($\pm 3\sigma$). Adding a full kilometer for Yarkovsky effect and solar pressure acceleration uncertainties, the error ellipse is still well within the desired 14 km target. Note that contribution of error (not just shifting the b-plane mean, but the spread of errors) from these two effects, if not already sufficiently reduced by 2017, can be further reduced from an application of the same batch filtering technique whereby parameters associated with the magnitude and direction of those effects can be added to both the propagation model as well as the optimization variable set. Note also that there is some margin in selecting a 300-day measurement arc. Should the mission be delayed or suffer a failure late in the mission, the goal of reducing the error ellipse $\pm 3\sigma$ distance (i.e. 6 times sigma) to under 14 km might still be satisfied.

G. Before and After Mission Distributions on the 2029 Encounter b-plane

Viewed in the 2029 b-plane centered on Earth, the proposed mission has a significant effect on reducing the error ellipse. The new error ellipse prediction appears in Figure 14, along with the original error ellipse, for comparison. Axes are square in both the zoomed in and zoomed out views of the error ellipse. The “After Mission” error ellipse is shown in green superimposed on the initial distribution. The “Initial” distribution is obtained by propagating the current state of Apophis (circa 2005) with random normal distributions on the orbital elements taken from JPL’s Sentry database on Apophis using our internally developed orbital propagator. Note that this Initial orbit does not account for any subsequent optimal or radar observations. As discussed previously, the “After Mission” distribution likewise does not account for additional Earth-based observations.

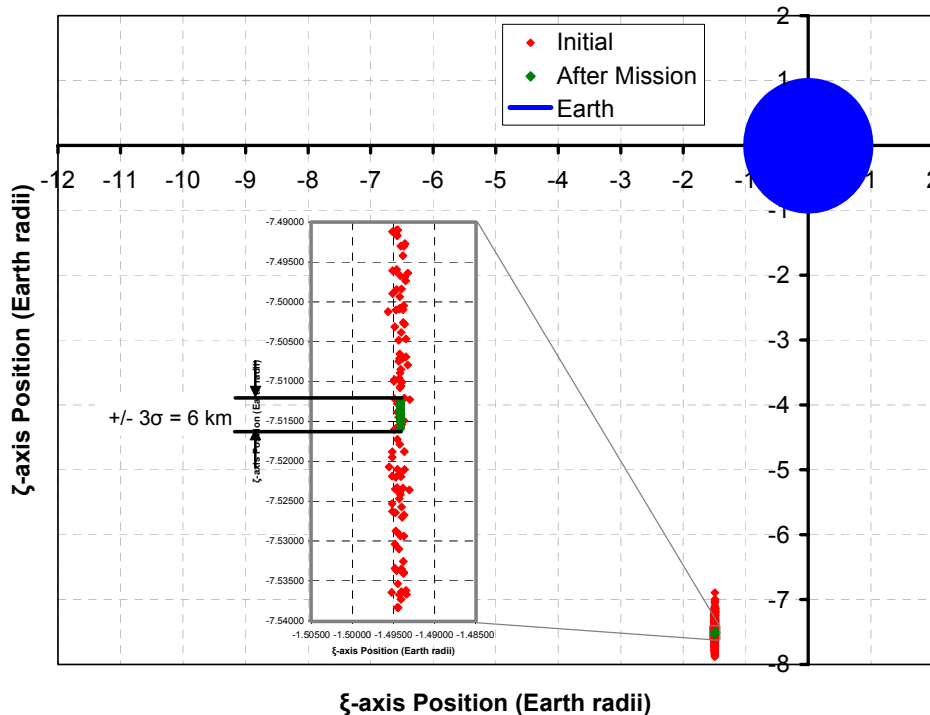


Figure 14. Initial and Final B-Plane Error Ellipse Comparison

While our goal is strictly to reduce the error ellipse in 2029 and not establish directly whether Apophis will pass through the 7:6 keyhole, it is clear that information such as that calculated for our proof-of-concept would be invaluable to future decision makers. Once a precise orbit is determined in early 2017, future decision makers will be able to plot this “actual” data on a 2029 b-plane to determine if it overlaps the 7:6 keyhole and to what degree. Should a significant danger exist, there would still be sufficient time to mount a deflection mission or take appropriate mitigation steps.

III. Spacecraft Design

A. Overall Spacecraft Design

The primary objective of the design of the spacecraft for the Foresight mission was to minimize life cycle cost. This objective led to an overall design philosophy emphasizing a simple, streamlined design using off-the-shelf components whenever possible. A minimalist approach was employed when selecting scientific payloads and subsystem components for the spacecraft: only those subsystems and equipment required to meet the mission objectives were included in the vehicle design. However, redundancy of critical hardware components was incorporated. In order to increase the flexibility of potential launch vehicles and decrease launch costs, the mission was designed for a launch into LEO. This required the spacecraft to be capable of performing both an Earth departure and Apophis arrival maneuver. Mass modeling showed that using a two stage vehicle offered a significant performance increase over a single stage vehicle, so a two stage vehicle was set as the baseline. This configuration is significantly less costly than employing an interplanetary launch vehicle, because the higher cost of an interplanetary launch vehicle would far outweigh the corresponding decreased costs due to reduced spacecraft propulsion requirements. The combined Foresight spacecraft and PTV is shown in Figure 15.

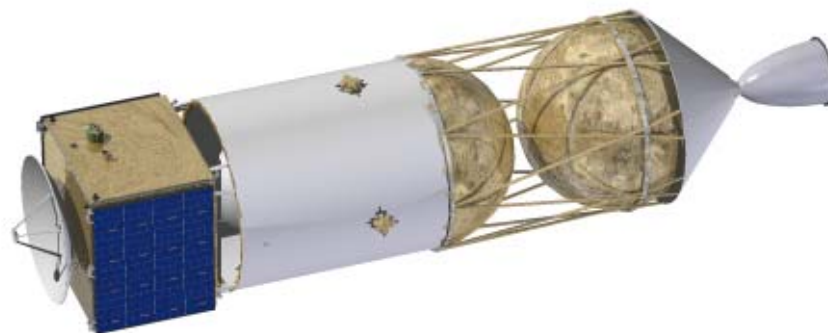


Figure 15. Foresight Encounter Spacecraft and PTV

The mass of the combined spacecraft at launch with growth margin is 1,607 kg. The reported payload capability of the Minotaur IV from the MARS is 1,680 kg, yielding a launch vehicle payload margin of 4.4% not including the 20% growth margin included in the vehicle masses themselves. The combined vehicle has a maximum effective diameter of 1.20 m and a length of 4.04 m. This is within the limits of the payload fairing of the Minotaur IV, which are 1.33 m in diameter and 4.62 m in length⁵. A view of the combined spacecraft inside the Minotaur IV payload fairing is shown in Figure 16.

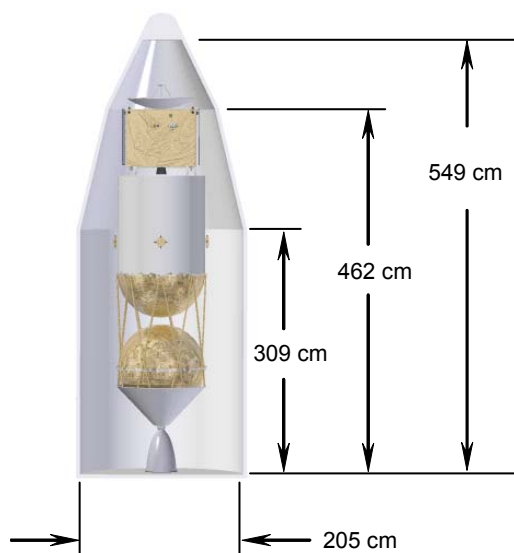


Figure 16. Foresight Encounter Spacecraft and PTV in Minotaur IV Payload Fairing

B. Foresight Encounter Spacecraft

1. Overview

The mission requirements of the Foresight Encounter Spacecraft include the ability to perform two transfer trajectory maneuvers and operate in the vicinity of Apophis for up to one year. The spacecraft needs to house scientific equipment sufficient to image the asteroid and provide accurate range measurements from the asteroid, and provide sufficient computational power and memory to store this data. During the near-Apophis operations, the spacecraft must be able to make precise velocity changes to maneuver about the asteroid. Finally, the spacecraft must communicate to Earth at all times at a low data rate, and occasionally download large amounts of data at a high data rate. The spacecraft was designed to accommodate all of these mission requirements; its overall design can be seen in Figures 17 and 18.

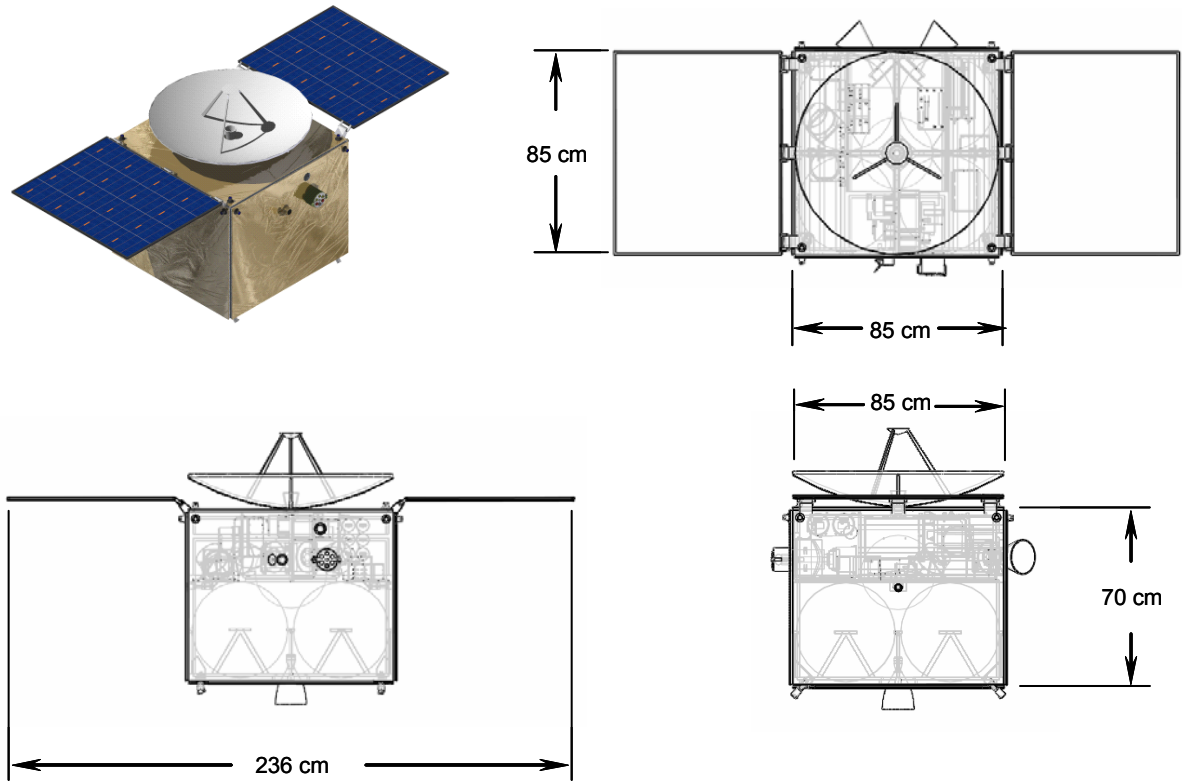


Figure 17. Foresight Encounter Spacecraft Dimensions

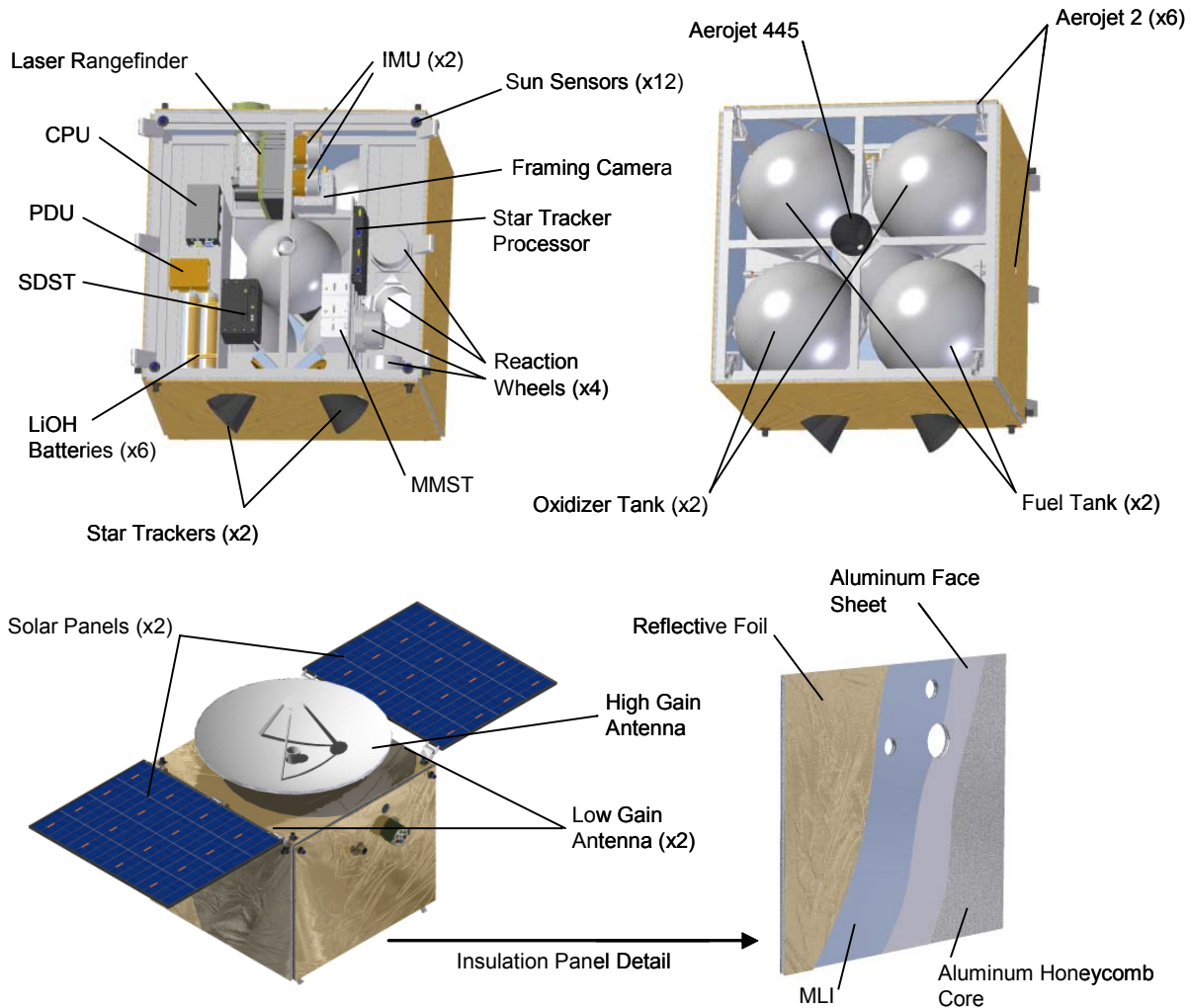


Figure 18. Foresight Encounter Spacecraft Detail

Primary power for the spacecraft is provided by two solar arrays. These arrays are folded against the sides of the vehicle during launch. A simple, 1-axis locking hinge mechanism is used to rotate the solar arrays 90° to their deployed position once the spacecraft has departed LEO. Once deployed, the solar arrays are fixed relative to the spacecraft body. During the Initial Survey and Tracking phases of the mission, the spacecraft will spend most of its time aligned as per Figure 3 with the solar arrays facing the Sun and the scientific instruments facing Apophis, allowing the solar arrays to provide all the vehicle power required. Similarly, during the Observation phase while the spacecraft is in Low Apophis Orbit, the spacecraft will be similarly with the solar arrays facing the Sun and scientific instruments facing the asteroid. This alignment is outlined in Figure 19. The solar arrays are augmented by a bank of six Li-Ion batteries. These batteries provide power during peak power loads and during communications phases when the spacecraft cannot be oriented for optimal solar array power generation.

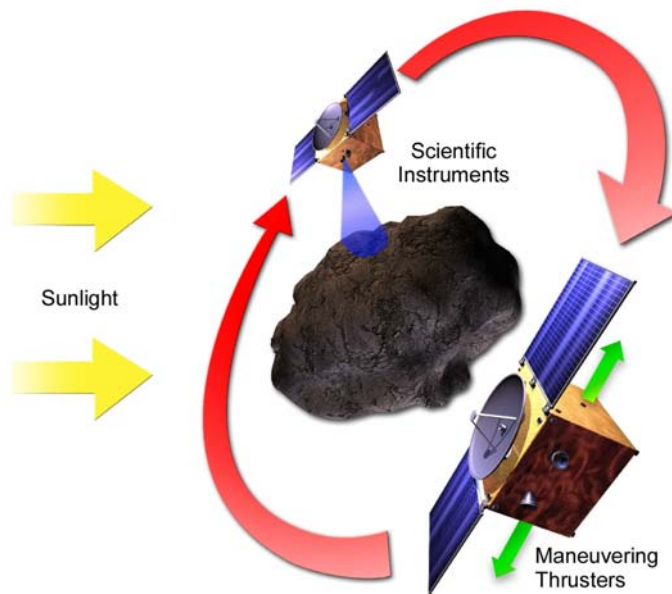


Figure 19. Alignment of Spacecraft Components during Observation Phase.

Communications to Earth are performed through a fixed high gain antenna and two low gain antennas. As seen in Figure 3, the Sun and Earth are always on the same side of the spacecraft, though the Earth's position varies from that of the Sun by up to 90° . The high gain antenna was therefore positioned to point in the same direction as the solar arrays to allow the solar arrays to continuously provide some amount of power during high data rate transmissions via the high gain antenna, augmented by the batteries.

The spacecraft propulsion system includes a main engine, six maneuvering thrusters, four propellant tanks, a pressurant tank, and associated feed lines and valves. The main engine performs the two main burns for Earth departure and Apophis arrival. On the same spacecraft body face as the main engine are four reaction control system (RCS) thrusters serving to provide attitude control during these maneuvers. The alignment of these four thrusters, as seen in Figure 20 is such that firing adjacent pairs gives moment about the two axes parallel to that spacecraft face, and firing diagonal pairs gives moment about the axis normal to that face, while firing all four gives moment-free force in the same direction as the main engine. The remaining two thrusters are the translation thrusters serve as the primary vehicle propulsion for position maneuvering during the remainder of the mission. The alignment of these thrusters is through the spacecraft center of mass and in the direction parallel and anti-parallel to the vehicle velocity vector while in orbit about Apophis. This configuration allows the spacecraft to easily increase and decrease its Apophis orbital energy and modify its Low Apophis Orbit as shown in Figure 20.

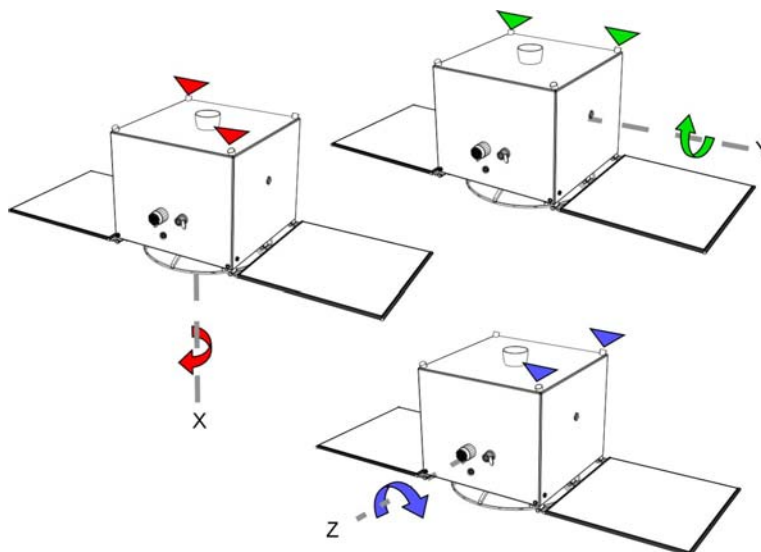


Figure 20. Generation of Moments about X, Y, and Z axes with four maneuvering thrusters on propulsion face.

During the two main engine burns, attitude control of the ES is provided by the four RCS thrusters. Otherwise, attitude control is maintained by four reaction wheels. Nominally, the three wheels aligned with spacecraft body XYZ axes will be used. The 4th wheel, on a skew axis, will be reserved as a spare which can maintain three-axis control in case of a failure of one of the nominal wheels. The four RCS thrusters can be used to de-saturate the reaction wheels. Attitude determination is performed with a combination of measurements from Sun sensors, star trackers, and the fiber-optic gyros (FOGs) in the IMU, integrated by an Extended Kalman Filter (EKF)¹³. The EKF will be a model-replacement version, where the traditional dynamics model is replaced by gyro angular rate measurements. The ES houses two star trackers and twelve Sun sensors. The Sun sensors are such that each face has a sensor able to detect the sun despite shadowing caused by the solar arrays and high gain antenna, with four on the communications face and two on each of the four adjacent faces. The two star trackers give redundancy, and also eliminate the lower level of accuracy that a single star tracker has about its boresight.

All of the subsystems inside the ES are enclosed in an 85 cm x 85 cm x 70 cm box wrapped in multilayer insulation (MLI) and a reflective foil to maintain thermal control. In addition, the spacecraft contains several small resistive Kapton heaters to keep component temperatures from dropping too low. The outer box also serves as the vehicle's primary structure. Internal structure including fasteners and attachment points is used to secure the internal hardware.

A mass breakdown statement for the ES is presented in Table 3.

Table 3. Encounter Spacecraft Mass Breakdown Statement

No.	Name	Element Mass [kg]	Subsystem Mass [kg]
1.0	Structures and Mechanisms		26.0
	Primary Structure	14.8	
	Secondary Structure	5.5	
	Fuel Tank	2.3	
	Oxidizer Tank	2.3	
	Pressurant Tank	0.7	
	Solar Array Support Structure	0.2	
	Solar Array Actuators	0.2	
2.0	Propulsion		7.0
	Main Engine: Aerojet 445	1.9	
	Main Engine Feed Lines	1.9	
	Maneuvering Engines: Aerojet 2 (x4)	1.6	
	Maneuvering Engine Feed Lines	1.6	
3.0	Thermal Control		5.0
	Reflective Foil	1.0	
	Multi-Layer Insulation	3.8	
	Heaters	0.2	
4.0	Power		12.1
	Batteries: Saft VES 180 (x6)	6.7	
	Solar Array: Spectrolab Triple Junction	2.1	
	Power Distribution Unit	1.7	
	Power Cabling	1.6	
5.0	Command and Data Handling		4.9
	CPU: PowerPC 750FX	0.1	
	Memory: Samsung 64 GB Solid State Drive (x2)	0.1	
	Electronics Module	1.0	
	Wiring	3.7	
6.0	Attitude Determination and Control		12.9
	Sun Sensors: AeroAstro MSS (x6)	0.4	
	Star Sensors: Terma HE-5AS (x2)	4.4	
	Reaction Wheels: Dynacon MicroWheel 1000	6.6	
	Inertial Measurement Unit: LN-200S	1.5	
7.0	Communications		8.9
	High Gain Antenna	3.0	
	Low Gain Antenna (x2)	0.7	
	Small Deep Space Transponder	2.9	
	Multi-Mode S-Band Transceiver	2.3	
8.0	Margin		13.6
9.0	Dry Mass		90.2
10.0	Consumables		120.1
	Fuel: MMH	45.1	
	Oxidizer: NTO	74.4	
	Pressurant: He	0.7	
12.0	Wet Mass		210.3
13.0	Payload		10.0
	Advanced Imagery Mechanism (AIM)	5.0	
	Laser Altimeter Device (LAD)	5.0	
14.0	Gross Mass		220.3

2. Scientific Instrument Suite

There is a minimum suite of science instruments in this mission. Inclusion of any instruments is predicated upon their necessity to the overall science objective, with a view toward limiting mission cost and complexity. Thus, there are two primary instruments on the spacecraft: the Advanced Imagery Mechanism (AIM), and the Laser Altimeter Device (LAD).

The primary science goal of the AIM is to develop surface imagery of asteroid Apophis that will aid in determination of size, shape, and surface/regolith features. Data from AIM will also assist in development of asteroid mass estimates. The AIM will be assumed to have heritage from previous spacecraft missions, specifically based upon the framing camera of the Dawn asteroid mission¹⁴. The AIM consists of a camera head, CCD, filter wheel, and associated electronics. Radiation hardened optics will pass incoming light through a filter wheel onto a 1024x1024 CCD. Focal length is 150 mm, Field of View (FOV) is 5.5 degrees yielding a resolution of 9.3 m/pixel at

a distance of 100 km. A multi-spectral filter wheel will be on the instrument. The range of the filters is assumed to be similar to those from previous missions including Deep Impact, Contour, Hayabusa, and Dawn^{14,15,16,17}. There is anticipated to be one clear filter and seven filters ranging from 450 to 980 nm (450, 540, 650, 750, 830, 920, and 980 nm). Anticipated mass for the camera is 5 kg, consuming 12 W.

The primary science goal of the LAD is to use reflected laser measurements from asteroid Apophis to determine distance, shape, internal structure (when combined with accurate spacecraft trajectory data), and surface topography. The laser altimeter (or LIDAR) will use a neodymium-yttrium-aluminum-garnet (Nd-YAG) laser. This laser altimeter system will be similar to other instruments used on previous spacecraft such as NEAR Laser Rangefinder (NLR) on NEAR, Light Detection and Ranging Instrument (LIDAR) on Hayabusa, and the Lunar Orbiter Laser Altimeter (LOLA) on the Lunar Reconnaissance Orbiter (LRO)^{17,18,19}. The range requirement for the LAD will be 50 km and designed for low albedo, diffusely reflecting surfaces present on asteroids¹⁸. The LAD consists of two separate units: a laser transmitter and a telescope receiver/photo detector. Both the AIM and the LAD will be boresighted such that visual imagery and laser ranging data can complement each other. It is anticipated that the LAD will be able to fire multiple times per minute, returning and firing several million times over the course of the instrument's lifetime. Anticipated mass for the laser altimeter is 5 kg, consuming 20 W (peak) and 15 W (average).

3. Detailed Subsystem Description

Many of the subsystems will be based upon flight systems and experience of satellite/subsystem developer and project team member SpaceDev, Inc. Where available, flight proven subsystems will be utilized in order to provide higher certainty of mission success. In addition, manufacturers of the relevant subsystems have been identified where possible. A list of the individual subsystem components selected for this mission is provided in Table 4.

The structure housing for the Foresight spacecraft is composed of Teklam Aluminum honeycomb panels²⁰. Panels of varying thickness are used depending on the structure loads on the panels. Internally, the thermal control of the spacecraft is designed for a cold bias. Unattended, the subsystems in the spacecraft will operate below their intended operating ranges, so heaters are used to maintain the subsystems at their operating temperatures. In addition, the spacecraft exterior is covered in several blankets of Multilayer Insulation (MLI) and an outer layer of reflective foil to marginalize the impact of solar radiation on the thermal environment inside the spacecraft.

A particular strength of the spacecraft design is its modern flight software architecture. The flight software will be very high performance, taking advantage of the main computer's high processing power, and making extensive use of pre-existing software modules. This approach is in contrast to that of traditional spacecraft, which often employ unique software elements for every mission, incurring much greater costs without corresponding increases in performance. Characteristics of the flight software include the following: highly modular, reusable C++ code throughout, Commercial Off-The-Shelf (COTS) code for increased performance and decreased cost, embedded LINUX operating system with fault-tolerant boot loader (redundant flight images), software modules configured with XML files for easy reconfigurability, Ethernet connection between bus and payloads (Internet Protocol routed from ground to payloads), data transfers to and from spacecraft via FTP, web-based command and control of the satellite bus, and ground terminal able to act as remote telnet console to the spacecraft bus or payloads.

A power budget for the Foresight spacecraft is presented in Table 5. Power Conversion/Conditioning Loss is assumed to be 5.0% and cabling losses 0.5%. This yields an overall end-to-end solar array efficiency of 14.3% at the end of three years. The selected solar arrays have flight experience in LEO and to multiple planetary bodies²¹. Lithium-ion batteries from Saft are aboard the spacecraft for use during various mission phases including multiple propulsion phases and to be available during periods of array/asteroid shading when performing proximity operations near Apophis²².

Table 4. Subsystem Component Specifications.

Component	Name	Manufacturer	No. on ES	No. on PTV	Specifications
Propulsion					
S/C Main Engine ²²	Aerojet 445	Aerojet	1	0	Thrust (vac): 445 N, Isp: 309 s, T/W: 24.39
S/C RCS ²³	Aerojet 2	Aerojet	1	0	Thrust (vac): 2 N, Isp: 265 s, T/W: 0.75
PTV Main Engine ²⁴	R-40B	Aerojet	0	1	Thrust (vac): 4000 N, Isp: 293 s, T/W: 56.4
PTV RCS ²⁵	Aerojet 21	Aerojet	0	1	Thrust (vac): 21 N, Isp: 285 s, T/W: 3.81
Thermal Control					
Heaters ²⁶	Kapton Heaters	Minco	16	0	-200 to 200°C range, Kapton/FEP material
Power					
Batteries ²¹	VES 180	Saft	6	2	Li-Ion space technology, specific energy: 165 Wh/kg, storage: 180 Wh each
Solar Array ²²	Triple Junction	Spectrolab	2	0	GaNP2/GaAs/Ge, BOL power: 289 W/m2, BOL efficiency: 22.5%, EOL power: 256 W/m2, 4% degradation per year
Distribution	PDU	SpaceDev	1	1	x
Command and Data Handling					
CPU ²⁷	PowerPC 750 FX	IBM	1	0	RISC Microprocessor, 1856 MIPS at 800 MHz with 256 MB RAM, RS-422 / USB / Ethernet compatible
Memory ²⁸	16 GB SSD	Samsung	2	0	NAND-based SSD, read rate: 57 MBps, write rate: 32 MBps
SCC ²⁹	8051	Silicon Labs	0	1	1000 MIPS @ 100 MHz, 128 KB Flash, 8448 bytes data RAM, 8 12-bit ADCs, 2 12-bit DACs
Attitude Determination and Control					
Sun Sensor ³⁰	MSS	AeroAstro	12	0	60° FOV, accuracy ±1°
Star Tracker ³¹	HE-5AS	Terma	2	0	22° FOV, <1 arcsec cross-track accuracy, 5 arcsec boresight accuracy
Reaction Wheel ³²	MicroWheel 1000	Dynacon	4	0	Produce 30 mNm torque, hold 1000 mNm angular momentum, mounted with 1 each on XYZ axes and 1 on skew axis
IMU ³³	LN-200S	Grumman	1	1	Fiber Optic Gyro, silicon accelerometers and electronics
Communications					
Low Gain Antenna ³⁴	Custom	Ball Aerospace	2	0	S-Band, 50 bps data rate
High Gain Antenna ³⁴	Custom	Ball Aerospace	1	0	X-Band, 17 kbps data rate at 0.5 AU, SNR: 3, efficiency: 55%
X-Band Transponder ³⁵	SDST	General Dynamics	1	0	DSN Compatible, X-Band transmit and receive, 2.0 dB Noise Figure, -157.7 dBm Receiver Threshold, 10 ns Ranging Delay Variation, 0.5 ns Carrier Delay Variation
S-Band Transceiver ³⁶	Multi-Mode S-Band Transceiver	General Dynamics	1	0	DSN Compatible, S-Band transmit and receive, < 2.5 dB Noise Figure, Delay Variation, 0.5 ns Carrier Delay Variation

Table 5. Power Budget for Foresight Spacecraft (all values in W).

Subsystem Name	Max. Power Requirement	Power for Various Operating Modes									
		Standby	Earth Departure Maneuver	Commissioning	Cruise	Rendezvous Maneuver	Initial Survey	Image Transmission	At-Apophis Maneuvers	Observation	Tracking
Main Engine	20.0	0.0	20.0	20.0	0.0	20.0	0.0	0.0	0.0	0.0	0.0
RCS Thrusters	18.0	0.0	18.0	18.0	18.0	18.0	0.0	0.0	18.0	0.0	0.0
Heaters	30.0	0.0	30.0	30.0	30.0	30.0	30.0	30.0	30.0	30.0	30.0
Power Distribution	5.0	5.0	5.0	5.0	5.0	5.0	5.0	5.0	5.0	5.0	5.0
CPU	4.0	4.0	4.0	4.0	4.0	4.0	4.0	4.0	4.0	4.0	4.0
Memory	0.5	0.5	0.5	0.5	0.5	0.5	0.5	0.5	0.5	0.5	0.5
Sun Trackers	0.0	0.0	0.0	0.0	0.0	0.0	0.0	0.0	0.0	0.0	0.0
Star Trackers	13.6	0.0	13.6	13.6	13.6	13.6	13.6	13.6	13.6	13.6	13.6
Reaction Wheels	20.0	0.0	0.0	0.0	0.0	0.0	20.0	20.0	20.0	20.0	20.0
IMU	12.0	12.0	12.0	12.0	12.0	12.0	12.0	12.0	12.0	12.0	12.0
Low Gain Antenna	10.0	10.0	10.0	10.0	10.0	10.0	10.0	10.0	10.0	10.0	10.0
S-Band Transponder	5.0	5.0	5.0	5.0	5.0	5.0	5.0	5.0	5.0	5.0	5.0
High Gain Antenna	20.4	0.0	0.0	0.0	0.0	0.0	0.0	20.4	0.0	0.0	0.0
X-Band Transponder	14.1	0.0	0.0	0.0	0.0	0.0	0.0	14.1	0.0	0.0	0.0
Solar Array Actuators	20.0	0.0	0.0	20.0	0.0	0.0	0.0	0.0	0.0	0.0	0.0
Total Power Without Payload	177.6	41.5	103.1	123.1	103.1	103.1	105.1	139.6	123.1	105.1	105.1
Payload 1: AIM	12.0	0.0	0.0	0.0	0.0	12.0	12.0	0.0	12.0	12.0	12.0
Payload 2: LAD	15.0	0.0	0.0	0.0	0.0	15.0	15.0	0.0	15.0	15.0	15.0
Total Baseline Power Required	204.6	41.5	103.1	123.1	103.1	130.1	132.1	139.6	150.1	132.1	132.1
Power Conversion/Conditioning	10.2	2.1	5.2	6.2	5.2	6.5	6.6	7.0	7.5	6.6	6.6
Cabling Losses	1.0	0.2	0.5	0.6	0.5	0.7	0.7	0.7	0.8	0.7	0.7
Total Without Margin	215.8	43.8	108.8	129.9	108.8	137.3	139.4	147.2	158.4	139.4	139.4
Margin %	64.7	13.1	32.6	39.0	32.6	41.2	41.8	44.2	47.5	41.8	41.8
Total With Margin	280.6	56.9	141.4	168.8	141.4	178.4	181.2	191.4	205.9	181.2	181.2

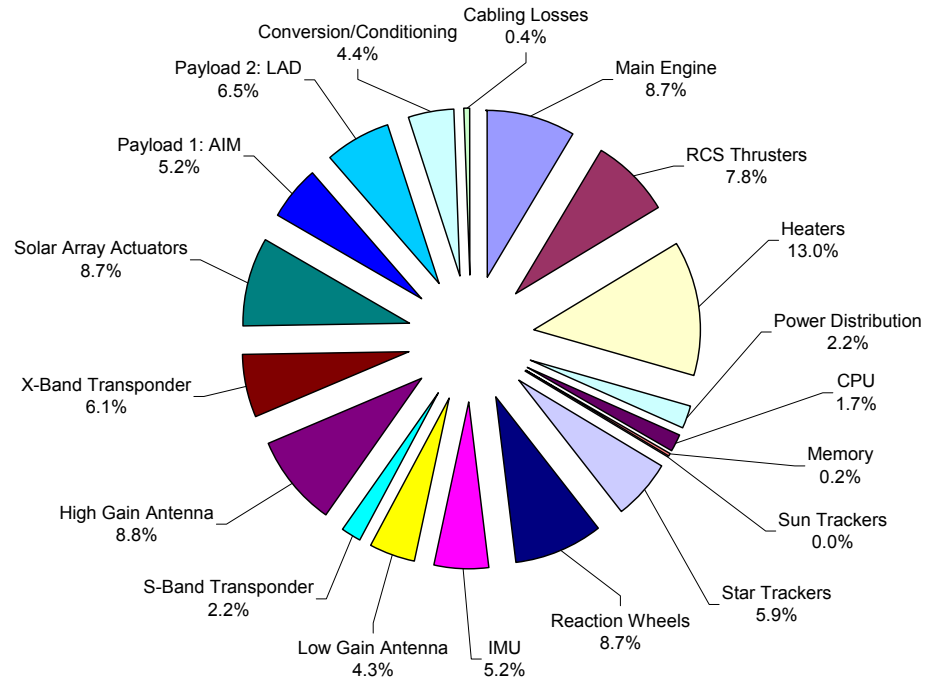


Figure 21. Average Power Requirement of Components in Foresight Spacecraft [215.6 W Total]

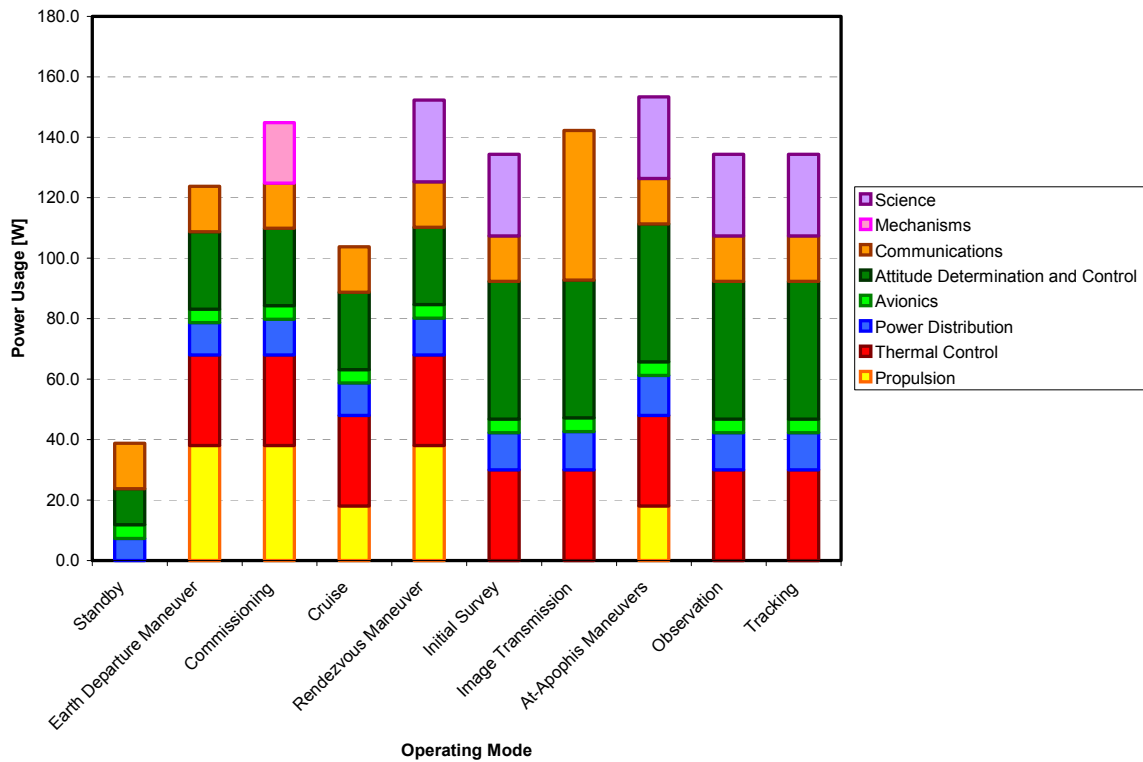


Figure 22. Power Levels for Different Foresight Spacecraft Operating Modes

C. Propulsive Transfer Vehicle (PTV)

The Propulsive Transfer Vehicle is a simple upper-stage type bi-propellant rocket stage used to propel the Foresight vehicle onto its Trans-Apophis Trajectory. The PTV is activated immediately after the final stage of the Minotaur IV launch vehicle is spent and fires continuously until it has consumed nearly its entire stock of propellants. Afterwards, it is separated from the ES and discarded. The design of the PTV is shown in Figure 23.

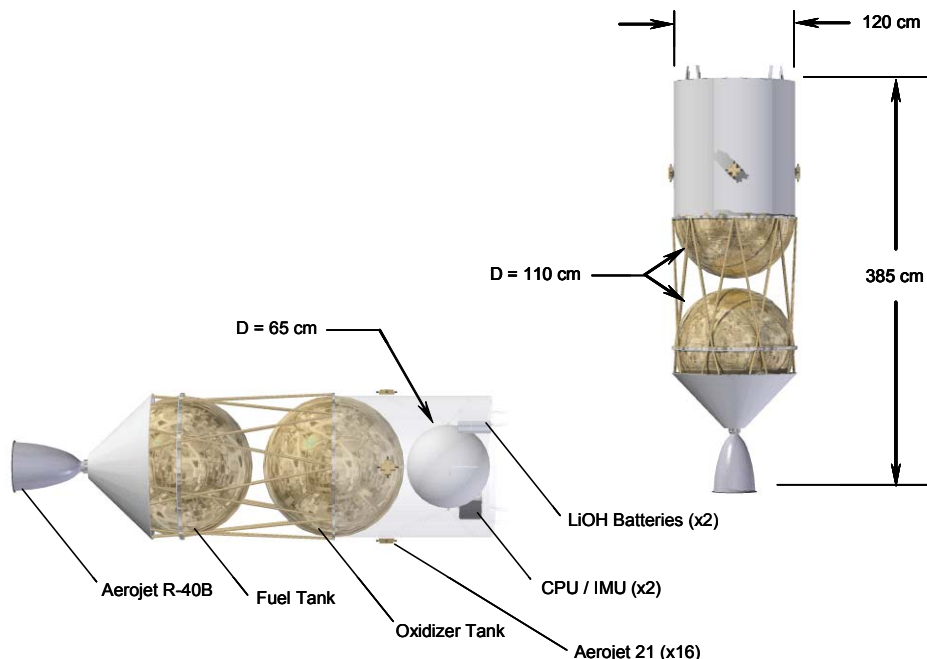


Figure 23. Propulsive Transfer Vehicle (PTV) Dimensions

The main engine of the PTV is an Aerojet R-40B bipropellant spacecraft propulsion engine using identical propellants as the ES (MMH/NTO). This engine is currently in production and will be available off-the-shelf for the PTV design²⁵. Attitude control is maintained during the PTV main engine burn by four sets of quad Aerojet 21 bipropellant RCS thrusters, also currently in production²⁵. As with the ES, the main engine and RCS thrusters both draw from a common fuel and oxidizer tank. Pressure is provided to the system by a single Helium tank pressurized to 400 psia at the start of the mission.

The PTV is powered by a pair of Saft VES 180 batteries providing a total of 360 W-hrs of electrical power storage. The power requirement of the PTV is 200 W during the transfer burn, which has a duration of 13.2 minutes. The 360 W-hrs of power capacity is more than sufficient for this vehicle. Guidance, navigation, and control of the PTV is performed by an onboard computer and LN 200-S inertial measurement unit in conjunction with the RCS thrusters.

The components of the PTV are housed inside a minimum-mass truss structure. The avionics ring, propellant and pressurant tanks, and engine thrust structure are all covered with multilayer insulation and a reflective material to provide thermal control during the brief lifetime of the vehicle. The R-40B includes an ablative nozzle removing the need for any active thermal control system.

The mass breakdown statement for the PTV is presented in Table 6. An additional 2.5% of the fuel and oxidizer are carried as reserves and residuals, and the tank volumes were increased by 2.5% to account for ullage in the tanks.

Table 6. Propulsive Transfer Vehicle Mass Breakdown Statement

No.	Name	Element Mass [kg]	Subsystem Mass [kg]
1.0	Structures		133.6
	Primary Structure	18.8	
	Secondary Structure	13.9	
	Payload Adapter	5.5	
	Fuel Tank	22.5	
	Oxidizer Tank	22.7	
	Pressurant Tank	50.2	
2.0	Propulsion		31.8
	Main Engine: Aerojet R-40B	6.8	
	Main Engine Feed Lines	6.8	
	RCS Engines: Aerojet 21 (x16)	9.1	
	RCS Engine Feed Lines	9.1	
3.0	Thermal Control		12.1
	Reflective Foil	2.4	
	Multi-Layer Insulation	9.7	
4.0	Power		6.2
	Batteries: Saft VES 180 (x2)	2.2	
	Power Distribution Unit	0.9	
	Wiring	3.1	
5.0	Command and Data Handling		1.6
	Spacecraft Control Computer	0.1	
	Electronics Module	1.0	
	Wiring	0.5	
6.0	Attitude Determination and Control		1.5
	Inertial Measurement Unit: LN-200S	1.5	
7.0	Margin		37.4
8.0	Dry Mass		224.2
9.0	Consumables		1,163.1
	Fuel: MMH	426.1	
	Fuel Reserves / Residuals	10.5	
	Oxidizer: NTO	702.7	
	Oxidizer Reserves / Residuals	17.3	
	Pressurant: He	6.5	
10.0	Wet Mass		1,387.3
11.0	Payload		220.3
	Foresight Spacecraft	220.3	
12.0	Gross Mass		1,607.6

D. Reliability Assessment

A high probability of Foresight mission success is achieved due to simplicity of design, the use of proven components, and design redundancy. Results of a reliability analysis for the Foresight mission yields a mean mission success probability of 90.2 percent. Stated alternatively, loss of mission (LOM) is expected to occur only once every 10.2 missions. The 90th percentile value for mission success is 89.4 percent. Mission success, for the purposes of this reliability analysis, was defined as proper functioning of the launch vehicle, PTV, spacecraft, and instrument set to determine Apophis' orbit according to the design competition rules. Figure 24 shows the resulting probability distribution for mission success.

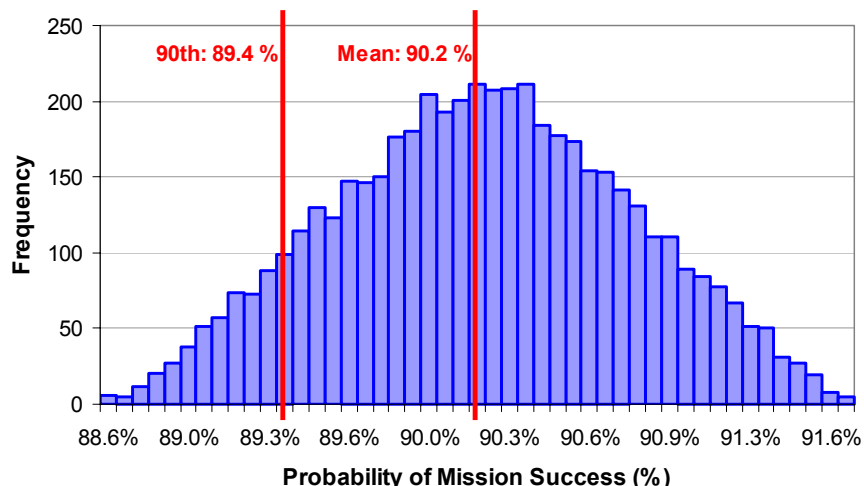


Figure 24. Histogram of Reliability Results (20,000 Monte Carlo Trials).

The relative contribution of each architecture element to the LOM end state is shown in Figure 25. Failure of the Minotaur-4 launch vehicle to insert the PTV and ES into the proper Earth departure trajectory is the leading cause of LOM with a total probability of failure of 5.2 percent. The ES has approximately a 3.2 percent probability of failure, primarily due to its lengthy worst-case operation time of 730 days. This worst-case probability decreases if an alternate launch window with a shorter cruise time is selected, or if the tracking phase is reduced to the minimum required 250 days rather than the more conservative 300 day period. Failure of the instruments and failure of the PTV each have less than a one percent mean probability of occurrence. The PTV is a simple propulsive stage using a proven engine and off-the-shelf electronic components. The LAD imager has a relatively high per hour failure rate, but is only needed during the initial survey and observation phases resulting in a moderate probability of failure. After the mass and rotation properties of the asteroid have been characterized by the LAD in the observation phase, the AIM altimeter alone can suffice to accurately determine the distance between the ES and Apophis during the tracking phase.

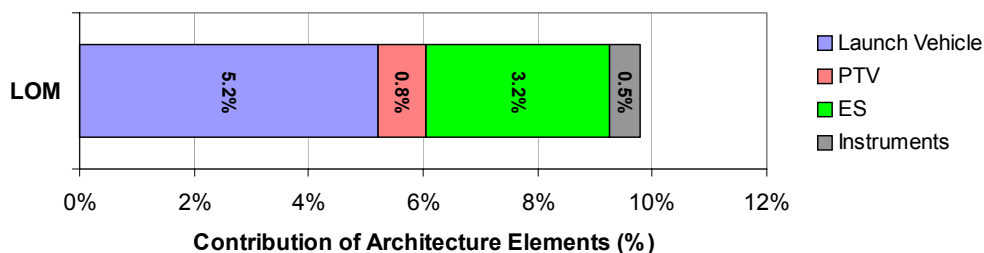


Figure 25. Contribution of Architecture Elements to LOM.

Reliability analysis was performed using a NASA standard fault tree and event sequence diagram approach as described in the NASA Probabilistic Risk Assessment Procedures Guide.³⁷ Basic events that might cause a loss of mission identified in calculation of Foresight mission reliability include structural failures, electronic hardware failures, mechanical failures, and failures due to the environment. Both the staging of the ES from the PTV and the deployment of solar arrays actions were included in the model. Environment failures include inability to launch during the available launch windows, damage to the spacecraft by micro-meteoroid impact, and electronics upset event due to radiation. Fault tree hardware basic events were predominantly at the component level, and continuous operating time reliability functions ($R=1-e^{-\lambda t}$) were applied for subsystems with significant operating times. Component redundancy was modeled through the use of logical “AND” and “N of M” gates where appropriate. Probabilistic results were generated from 20,000 Monte Carlo trials with symmetric triangular distributions of plus or minus 30 percent on the input variables.

Data sources for component failure rate values include commercial manufacturer publications, personal contact with manufacturers, SEI internal models, and technical papers of NASA and other professional organizations. The redundancies and failure rates of all Encounter Spacecraft components are given in Table 7. A similar redundancy approach and identical equipment was employed for the PTV, so those values are not repeated in this table. The Minotaur launch vehicle reliability was calculated using an approach similar to that previously employed by The Aerospace Corporation and Futron Corporation.³⁸ Whenever possible, manufacturer provided failure rate data was used for spacecraft electronic components. For electronic equipment where such data was unavailable, a default mean time between failures of one million hours was used. Component-level data was difficult to come by for communications equipment, so the failure rate for this subsystem was estimated at the subsystem level from a prior study of failures in historical communications and Earth observing spacecraft.³⁹ The failure rate of the LAD altimeter instrument was determined from a compilation of commercially available airborne laser altimeters and goals of the NASA Laser Risk Reduction Program.⁴⁰ The failure rate for the AIM camera is derived from the KOMPSAT-2 MSC imager.⁴¹

Table 7. Encounter Spacecraft Hardware Redundancy and Failure Rates

Element	Redundancy	Mean Time Between Failures per Unit or Failure Probability	Data Source
Encounter Spacecraft			
Structure and Tanks	Single	$P_f = 0.0012$	SEI internal est.
Main Engine: Aerojet 445	Single	$P_f = 0.002$	Small engine data
RCS/ACS	3 of 4	$P_f = 0.0014$	SEI internal est.
Passive TCS	Single	$P_f = 0.002$	Conservative est.
Heaters (two sets of 8)	Dual	MTBF = 1×10^6 hrs	Default value
Power Distribution and Regulation	Dual	MTBF = 1×10^6 hrs	Default value
Batteries: Saft VES 180	4 of 6	MTBF = 1×10^6 hrs	Default value
Solar Arrays	Dual*	$P_f = 0.001$	SpectroLab ²¹
CPU: PowerPC 750FX	Single**	MTBF = 2.5×10^6 hrs	IBM ⁴²
Memory: Samsung 32 GB Solid State Drive	Dual*	MTBF = 2×10^6 hrs	SanDisk ⁴³
Communications Subsystem	Dual***	MTBF = 3.1×10^6 hrs	Historical average ³⁹
Sun Sensors: AeroAstro MSS	Dual	MTBF = 1×10^6 hrs	Default value
Star Tracker: Terma HE-5AS	Dual	MTBF = 0.7×10^6 hrs	Terma ⁴⁴
Reaction Wheels: Dynacon MicroWheel1000	3 of 4	MTBF = 1×10^6 hrs	Default value
Inertial Measurement Unit: LN-200S	Dual	MTBF = 0.15×10^6 hrs	Northrop Grumman ⁴⁵
Instrument Package			
LAD Altimeter	Single	MTBF = 3.35×10^6 hrs	Analogy ⁴⁰
AIM Camera	Single	MTBF = 0.29×10^6 hrs	MSC derived ⁴¹

* Degraded performance after a single failure, but does not cause LOM

** Software fault tolerance only

*** X-band is single point failure but necessary during observation phase only; S-band is dual redundant

Successful Apophis orbit determination will require use of the Deep Space Network as discussed in Section II of this report. Uncertainty in DSN range measurements are accounted for in the proposed orbit prediction method and batch filtering algorithm, and thus this particular uncertainty does not have any additional contribution to LOM probability. Failure in the DSN causing its unavailability could lead to LOM, however, this unavailability would have to be prolonged (months) since duration of time to conduct measurements is more important than the frequency of those measurements as can be seen in Figure 12. Unavailability of the DSN for a measurement or even a series of measurements would still provide sufficient data to characterize the 2029 error ellipse. With this robustness inherent to the selected orbit characterization methodology and historical DSN availability on the order of 99%, the contribution to LOM by DSN is negligible.⁴⁶

E. Life-Cycle Cost (LCC) Analysis

A life cycle cost assessment has been performed for the Foresight concept design. The life cycle cost presented here includes Design, Development, Testing and Evaluation (DDT&E), acquisition cost, operations cost, and launch vehicle cost. All dollar units are in FY2007 constant U.S. dollars unless otherwise noted.

DDT&E and acquisition cost were determined using the NASA Air Force Cost Model (NAFCOM)⁴⁷. NAFCOM was set to use only weight-based Cost Estimating Relationship (CERs) based upon previous historical programs within the model's database. The historical missions that were used as analogies for each subsystem included the following NASA missions: Contour, Deep Impact flyby spacecraft, Genesis, Stardust, NEAR, and Lunar Prospector. For the PTV two additional data points were used: Orbital Maneuvering Vehicle (OMV) and Centaur-G primer liquid propulsion upper stage. Operations costs were determined using NASA's Spacecraft Operations Cost Model (SOCM)⁴⁸. Deep Space Network (DSN) costs were estimated using the NASA provided DSN Aperture Fee Tool⁴⁹. Spacecraft instrument costs were developed using a Jet Propulsion Lab (JPL) historical cost model⁵⁰. Launch vehicle costs for the Minotaur IV were assumed to be \$22M⁵¹.

A protoflight development plan was assumed, resulting in minimal System Test Hardware (STH). Extensive heritage was assumed for several subsystems including reaction control, attitude control, command and data handling, and thermal control. Existing engines were assumed for the PTV and Foresight spacecraft (resulting in no development cost). DDT&E and acquisition costs included programmatic sots such as Integration, Assembly, and Checkout (IACO), System Test Operations (STO), Ground Support Equipment (GSE), System Engineering & Integration (SE&I), and Program Management (PM). A 5% contractor development fee, 15% program support (NASA oversight), 30% contingency, and 4% vehicle integration total cost wraps were assumed.

The life cycle cost for this mission (including development and 4 years of operations) is estimated to be \$137.18 M (FY2007). Operations cost accounts for approximately \$21 M, a similar amount to the launch vehicle cost (see Table 8). This spacecraft's cost is similar to the costs for historical NASA Discovery class missions and particularly other previous asteroid missions (see Table 9). On a specific cost basis (\$M/kg) this spacecraft offers a very affordable solution, within the range of current small body missions.

Table 8. Life Cycle Cost Statement

Cost Element Name	DDT&E [FY2007]	Acquisition Cost [FY2007]	Total Cost [FY2007]
Spacecraft Stages	\$57.85 M	\$30.04 M	\$87.89 M
Foresight Encounter Spacecraft	\$23.51 M	\$14.77 M	\$38.28 M
Propulsive Transfer Stage (PTV)	\$34.34 M	\$9.27 M	\$43.61 M
Scientific Instruments (2)*	----	\$6.30 M	\$6.30 M
Operations	----	\$20.99 M	\$20.99 M
Operations: Flight	----	\$6.80 M	\$6.80 M
Operations: Nav&Track (DSN)	----	\$3.09	\$3.09 M
Operations: Science	----	\$1.70 M	\$1.70 M
Operations: Operations	----	\$9.40 M	\$9.40 M
Launch Vehicle: Minotaur IV	----	\$22.00 M	\$22.00 M
Total	\$57.85 M	\$79.33 M	\$137.18 M

* Note: AIM cost = \$3.71 M and university-developed LAD cost = \$2.59 M

Table 9. Spacecraft Cost Comparison^{52, 53}

Spacecraft Name	Spacecraft Cost [FY2007\$M]	Spacecraft Dry Mass [kg]	Cost to Mass Ratio [FY2007\$M/kg]
Clementine	\$80.16 M	235	\$0.341 M/kg
NEAR	\$123.67 M	480	\$0.258 M/kg
Mars Pathfinder	\$214.06 M	835	\$0.256 M/kg
Deep Space 1	\$106.06 M	279	\$0.380 M/kg
Mars Global Surveyor	\$141.54 M	674	\$0.210 M/kg
Dawn - original	\$343.50 M	740	\$0.464 M/kg
Dawn - w/overruns	\$446.00 M	740	\$0.603 M/kg
Foresight	\$87.89 M	314	\$0.280 M/kg

IV. Project Management Overview

SpaceWorks Engineering, Inc. (SEI) is the project lead for the submittal of this proposal to the Planetary Society. SpaceDev, Inc. is the main other team member for this project. In the event that the SpaceWorks Engineering, Inc. (SEI) / SpaceDev, Inc. team is awarded a cash prize or other award by the 2007 Apophis Mission Design Competition, it is agreed that 75% of the total prize or award shall be conferred to SpaceWorks Engineering, Inc. (SEI) and 25% of the total prize or award shall be awarded to SpaceDev, Inc.

Acknowledgments

The authors gratefully acknowledge the contributions of colleagues at SpaceWorks Engineering, Inc. (SEI) who contributed to this paper. Mr. Jon G. Wallace developed the computer-aided design (CAD) models used to help define the concept. Mr. Mark Elwood developed illustrations of the concept. Dr. John Bradford assisted in advice on multiple subsystems.

The authors also gratefully acknowledge the contributions of multiple colleagues at SpaceDev, Inc.

References

- 1: Anonymous, "Earth Impact Risk Summary, 99942 Apophis (2004 MN4)", URL: <http://neo.jpl.nasa.gov/risk/a99942.html>, [cited Oct 19, 2006].
- 2: Anonymous, "Projects: Apophis Mission Design Competition, Projects: Apophis Mission Design Competition Rules" URL: http://www.planetary.org/programs/projects/near_earth_objects/apophis_competition/rules.html [cited 31 August 2007].
- 3: Miller, J. K., et. al, "Determination of Shape, Gravity, and Rotational State of Asteroid 433 Eros", *Icarus* 155, 3-17 (2002)
- 4: Anonymous, "Orbital Sciences Corporation", URL: <http://www.orbital.com>, [cited 31 August 2007]
- 5: Anonymous, "Minotaur IV User's Guide", URL: http://www.orbital.com/NewsInfo/Publications/Minotaur_IV_Guide.pdf, [cited 31 August 2007]
- 6: Isakowitz, S. J., Hopkins, J. B., and Hopkins, J. P. Jr., *International Reference Guide to Space Launch System*, Fourth Edition, American Institute of Aeronautics and Astronautics, 2004.
- 7: Anonymous, "Chapter 3: General Performance Capabilities," *Eurockot User Guide*, Iss. 4, Rev. 0.
- 8: Chesley, Steven R., "Potential Impact Detection for Near-Earth Asteroids: The Case of 99942 Apophis (2004 MN4)," *Asteroids, Comets, Meteors Proceedings IAU Symposium*, No. 229, 2005.
- 9: Kinman, Peter W., *Sequential Ranging, DSN Telecommunications Link Design Handbook 810-005, Section 203, Rev. B*, Jet Propulsion Laboratory, 2007, URL: <http://deepspace.jpl.nasa.gov/dsndocs/810-005/203/203B.pdf>.
- 10: Valsecchi, G. B., Milani, A., Gronchi, G. F., and Chesley, S. R., "Resonant Returns to Close Approaches: Analytical Theory," *Astronomy and Astrophysics*, Vol. 408, pp. 1179-1196, 2003.
- 11: Anonymous, "Horizons User Manual," Version 3.12, January 2005, URL: http://ssd.jpl.nasa.gov/?horizons_doc
- 12: Vanderplaats, Garret N., *Numerical Optimization Techniques for Engineering Design*, Vanderplaats Research & Development, Inc., Colorado Springs, 1998.
- 13: Lefferts, E. J., Markley, F. L., Shuster, M. D., "Kalman Filtering for Spacecraft Attitude Estimation", *AIAA* 82-0070R, 1982.
- 14: Russel, C.T., et. al, "Dawn : A Journey to the Beginning of the Solar System", 2006.
- 15: Anonymous, "Deep Impact Legacy Site", URL: <http://deepimpact.jpl.nasa.gov/index.cfm>, [cited 27 August 2007].
- 16: Anonymous, "Discovery Mission: Countour", URL: <http://discovery.nasa.gov/contour.html>, [cited 27 August 2007].
- 17: Hayabusa Mission Reference
- 18: Anonymous, "NEAR Laser Rangefinder", John Hopkins University, URL: <http://near.jhuapl.edu>, [cited 27 August 2007].
- 19: Tooley, C. R., "Project Overview & Status, Lunar Reconnaissance Orbiter", NASA Goddard Space Center, URL: <http://lunar.gsfc.nasa.gov/>, [cited 27 August 2007].
- 20 : Anonymous, "FAA-Approved Aluminum Panels", URL: http://www.teklam.com/FAA_Approved_Panels.html, [cited 31 August 2007].
- 21: Anonymous, "Space Solar Panels Data Sheet," Spectrolab, URL: <http://www.spectrolab.com/DataSheets/Panel/panels.pdf>, [cited 31 August 2007].
- 22: Anonymous, "Li-Ion Batteries for Space", Saft Batteries, URL: http://saftbatteries.com/120-Techno/20-10_produit.asp?paramtechnolien=20-10_lithium_system.asp¶mtechno=Lithium+systems&Intitule_Produit=Spacelithium, [cited 31 August 2007].
- 22: Anonymous, "Aerojet 445", *Encyclopedia Astronautica*, URL: <http://www.astronautix.com/engines/aerjet445.htm>, [cited 31 August 2007].
- 23: Anonymous, "Aerojet 2", *Encyclopedia Astronautica*, URL: <http://www.astronautix.com/engines/aerjet2.htm>, [cited 31 August 2007].
- 24: Anonymous, "R-40B", *Encyclopedia Astronautica*, URL: <http://www.astronautix.com/engines/r40b.htm>, [cited 31 August 2007].
- 25: Anonymous, "Aerojet 21", *Encyclopedia Astronautica*, URL: <http://www.astronautix.com/engines/aerjet21.htm>, [cited 31 August 2007].
- 26: Anonymous, "Kapton™ Heaters", Minco, URL: <http://www.minco.com/products/heaters.aspx?id=71>, [cited 31 August 2007].
- 27: Anonymous, "PowerPC 750FX Microprocessor", IBM, URL: http://www-01.ibm.com/chips/techlib/techlib.nsf/products/PowerPC_750FX_Microprocessor, [cited 31 August 2007].
- 28: Anonymous, "Samsung Flash Solid-State Drive", Samsung, URL: <http://www.samsung.com/eu/Products/Semiconductor/products/ssd.asp>, [cited 31 August 2007].

- 29: Anonymous, "8051 Mixed-Signal Microcontrollers", Silicon Labs, URL: http://www.silabs.com/tgwWebApp/public/web_content/products/Microcontrollers/en/index.htm, [cited 31 August 2007].
- 30: Anonymous, "Medium Sun Sensor Data Sheet", AeroAstro, URL: <http://www.aeroastro.com/datasheets/MSS.pdf>, [cited 31 August 2007].
- 31: Anonymous, "The Terma Star Tracker", Terma, URL: <http://www.terma.com/index.dsp?page=1131#>, [cited 31 August 2007].
- 32: Anonymous, "MicroWheel 1000", Dynacon, URL: http://www.dynacon.ca/index.php/product_19/ProdID/14.html, [cited 31 August 2007].
- 33: Anonymous, "LN-200 Fiber Optic Inertial Measurement Unit", Northrop Grumman, URL: <http://www.nsd.es.northropgrumman.com/Html/LN-200/>, [cited 31 August 2007].
- 34: Ronald W. Humble, Gary N. Henry, Wiley J. Larson, ed., Space Propulsion Analysis and Design Space Technology Series, McGraw-Hill, 1995.
- 35: Anonymous, "Small Deep Space Transponder Data Sheet", General Dynamics, URL: www.gd-ais.com/Capabilities/offerings/space/datasheets/SDST.pdf, [cited 31 August 2007].
- 36: Anonymous, "Multi-Mode S-Band Transceiver", General Dynamics, URL: www.gd-ais.com/Capabilities/offerings/space/datasheets/MMS-BandXCVR.pdf, [cited 31 August 2007].
- 37: Stamatelatos, M., "Probabalistic Risk Assessment Procedures Guide for NASA Managers and Practitioners," NASA Office of Safety and Mission Assurance, NASA Headquarters, Washington, D.C., Version 1.1, Aug. 2002.
- 38: "Design Reliability Comparison for SpaceX Falcon Vehicles," Futron Corporation, November 2004.
- 39: "Spacecraft Reliability," RAMS Engineering [online website], Delft University of Technology, URL: <http://www.lr.tudelft.nl/live/pagina.jsp?id=9f3aa457-e8d4-4919-8054-6058facd48ba&lang=en> [cited 17 August 2007].
- 40: Meadows, B., Amzajerdian, F., Barnes, B., Kavaya, M., Singh, U., et. al. "Improving Reliability of Long Pulsewidth High Power Laser Diode Pump Arrays," 2005 Earth-Sun System Technology Conference [presentation charts], Maryland, June 2005.
- 41: Kim, Y., Lee, D., Lee, C., Woo, S., Reliability Analysis of the MSC System," Journal of Astronomy and Space Science, Vol. 20, No. 3, August 2003, pp. 217-226.
- 42: "IBM Power PC 750FX RISC Microprocessor," Version 1.3, IBM, 28 August 2003.
- 43: "SanDisk Launches 2.5-Inch Solid State Drive," SanDisk Corporation Press Release [online website], 13 March 2007, URL: <http://www.sandisk.com/Corporate/PressRoom/PressReleases/PressRelease.aspx?ID=3732> [cited 16 August 2007].
- 44: Davidsen, P., "Terma Star Tracker Reliability," Terma A/S Space Division, Denmark, Personal Correspondence [received 30 August 2007].
- 45: "LN-200S Inertial Measurement Unit Product Details: Frequently Asked Questions" [online website], Northrop Grumman Corporation, URL: <http://www.ngnavsys.com/Html/LN-200S/index.htm> [cited 15 August 2007].
- 46: "Exhibit 300 for O&M (BY2008) / SMD – Deep Space Network (DSN)," Investment Funding and Performance Form submitted to OMB [online website], 1 February 2007, URL: http://www.nasa.gov/172125main_SMD_Deep_Space_Network_DSN_Publish_COMPLETE.htm [cited 16 August 2007].
- 47: Anonymous, "NAFCOM Overview," URL: http://ceh.nasa.gov/webhelpfiles/Appendix_N-NAFCOM_Overview.htm [cited 31 August 2007].
- 48: Anonymous, "Space Operations Cost Model (SOCM)," URL: <http://cost.jsc.nasa.gov/SOCM/SOCM.html> [cited 31 August 2007].
- 49: Anonymous, "DSN Aperture Fee Tool," URL: <http://deepspace.jpl.nasa.gov/advmiss/#discover> [cited 31 August 2007].
- 50: Warfeld, K., Roust, K., "The JPL Advanced Projects Design Team's Spacecraft Instrument Cost Model: an Objective, Multivariate Approach," First Annual Joint ISPA/SCEA International Conference Toronto, Ontario, Canada, June, 1998, URL: <http://trs-new.jpl.nasa.gov/dspace/bitstream/2014/19241/1/98-0533.pdf> [cited 31 August 2007].
- 51: Anonymous, "Small, Flexible, Low-Cost Earth Science Missions," URL: <http://deepspace.jpl.nasa.gov/advmiss/#discover> [cited 31 August 2007], June 30, 2006
- 52: Darren, D., "Ions to propel spacecraft on 3.2B-mile, eight-year journey," July 30, 2007, URL: <http://www.knoxnews.com/news/2007/jul/30/ions-to-propel-spacecraft-on32b-mile-eight-year/> [cited 31 August 2007].
- 53: Anonymous, "Fact Sheet: Dawn Investigating the "Dawn" of Our Solar System," URL: http://www.orbital.com/NewsInfo/Publications/Dawn_fact.pdf [cited 31 August 2007].